

Synthesis, Structures, and DFT Bonding Analysis of New Titanium Hydrazido(2–) Complexes

Thomas B. Parsons, Nilay Hazari, Andrew R. Cowley, Jennifer C. Green, and Philip Mountford*

Chemistry Research Laboratory, University of Oxford, Mansfield Road, Oxford OX1 3TA, U.K.

Received July 28, 2005

The reaction of 1,1-diphenylhydrazine with $\text{Ti}(\text{NMe}_2)_2\text{Cl}_2$ produced the monomeric terminal titanium hydrazido(2–) species $\text{Ti}(\text{NNPh}_2)\text{Cl}_2(\text{HNMe}_2)_2$ (**1**) in near-quantitative yield. The reaction of $\text{Ti}(\text{NMe}_2)_2\text{Cl}_2$ with the less sterically demanding ligand precursors 1,1-dimethylhydrazine or N-aminopiperidine gave the dimeric $\mu\text{-}\eta^2,\eta^1$ -bridged compounds $\text{Ti}_2(\mu\text{-}\eta^2,\eta^1\text{-NNMe}_2)_2\text{Cl}_4(\text{HNMe}_2)_2$ (**2**) and $\text{Ti}_2\{\mu\text{-}\eta^2,\eta^1\text{-NN}(\text{CH}_2)_5\}_2\text{Cl}_4(\text{HNMe}_2)_3$ (**3**). The X-ray structures of **2** and **3** showed the formation of $\text{N}\cdots\text{Cl}$ hydrogen bonded dimers or chains, respectively. The reaction of **1** with an excess of pyridine formed $[\text{Ti}(\text{NNPh}_2)\text{Cl}_2(\text{py})_2]_n$ (**4**, $n = 1$ or 2). The reaction of the *tert*-butyl imido complex $\text{Ti}(\text{N}^t\text{Bu})\text{Cl}_2(\text{py})_3$ with either 1,1-dimethylhydrazine or N-aminopiperidine again resulted in the formation of hydrazido-bridged dimeric complexes, namely $\text{Ti}_2(\mu\text{-}\eta^2,\eta^1\text{-NNMe}_2)_2\text{Cl}_4(\text{py})_2$ (**5**, structurally characterized) and $\text{Ti}_2\{\mu\text{-}\eta^2,\eta^1\text{-NN}(\text{CH}_2)_5\}_2\text{Cl}_4(\text{py})_2$ (**6**). Compounds **1** and **4** are potential new entry points into terminal hydrazido(2–) chemistry of titanium. Compound **1** reacted with neutral *fac*- N_3 donor ligands to form $\text{Ti}(\text{NNPh}_2)\text{Cl}_2(\text{Me}_3[9]\text{aneN}_3)$ (**7**), $\text{Ti}(\text{NNPh}_2)\text{Cl}_2(\text{Me}_3[6]\text{aneN}_3)$ (**8**), $\text{Ti}(\text{NNPh}_2)\text{Cl}_2\{\text{HC}(\text{Me}_2\text{pz})_3\}$ (**9**, structurally characterized), and $\text{Ti}(\text{NNPh}_2)\text{Cl}_2\{\text{HC}(\text{Bupz})_3\}$ (**10**) in good yields ($\text{Me}_3[9]\text{aneN}_3$ = trimethyl-1,4,7-triazacyclononane, $\text{Me}_3[6]\text{aneN}_3$ = trimethyl-1,3,5-triazacyclohexane, $\text{HC}(\text{Me}_2\text{pz})_3$ = tris(3,5-dimethylpyrazolyl)methane, and $\text{HC}(\text{Bupz})_3$ = tris(4-*n*-butylpyrazolyl)methane). DFT calculations were performed on both the model terminal hydrazido compound $\text{Ti}(\text{NNPh}_2)\text{Cl}_2\{\text{HC}(\text{pz})_3\}$ (**I**) and the corresponding imido compounds $\text{Ti}(\text{NMe})\text{Cl}_2\{\text{HC}(\text{pz})_3\}$ (**II**) and $\text{Ti}(\text{NPh})\text{Cl}_2\{\text{HC}(\text{pz})_3\}$ (**III**). The NNPh_2 ligand binds to the metal center in an analogous manner to that of terminal imido ligands (metal=ligand triple bond), but with one of the $\text{Ti}=\text{N}_\alpha$ π components significantly destabilized by a π^* interaction with the lone pair of the N_β atom. The NR ligand σ donor ability was found to be $\text{NMe} > \text{NPh} > \text{NNPh}_2$, whereas the overall ($\sigma + \pi$) donor ability is $\text{NMe} > \text{NNPh}_2 > \text{NPh}$, as judged by fragment orbital populations, Ti–N atom–atom overlap populations, and fragment-charge analysis. DFT calculations on the hydrazido ligand in a $\mu\text{-}\eta^2,\eta^1$ -bridging mode showed involvement of the $\text{N}=\text{N}$ π electrons in donation to one of the Ti centers. This TiN_2 interaction is best represented as a metallocycle.

Introduction

For over four decades the chemistry of transition metal complexes containing hydrazido ligands has generated considerable interest,^{1,2} particularly with regard to developing models for the biological fixation of molecular nitrogen.³ However, despite the many advances in the field, there remain few reports of terminal titanium (or indeed other

Group 4 metal⁴) terminal hydrazido(2–) complexes of the type $(\text{L})\text{Ti}=\text{NNR}_2$ where (L) represents a supporting ligand or ligand set and R is an alkyl or aryl group (note that reports of titanium hydrazido(1–) compounds $[(\text{L})\text{Ti}(\text{NR}'\text{NR}'_2)]_n$ are comparatively abundant).⁵ This situation contrasts strongly to the rather well-developed area of titanium imido chemistry.⁶

Binuclear titanium compounds containing bridging hydrazido(2–) ligands are fairly well established.^{2a,7} The earliest report of a *terminal* titanium hydrazido(2–) compound was by Wiberg and co-workers in 1978⁸ for the pseudo-three-coordinate titanocene complex, $\text{Cp}_2\text{Ti}\{\text{NN}(\text{SiMe}_3)_2\}$. In 1999, we described the synthesis and $[2\pi + 2\pi]$ cycloaddition reactions of the macrocycle-supported $\text{Ti}(\text{NNPh}_2)(\text{Me}_n\text{taa})$

* To whom correspondence should be addressed. Email: philip.mountford@chem.ox.ac.uk.

(1) For reviews of transition metal hydrazido chemistry, see: (a) Sutton, D. *Chem. Rev.* **1993**, 93, 995. (b) Johnson, B. F. G.; Haymore, B. L.; Dilworth, J. D. In *Comprehensive Coordination Chemistry*; Wilkinson, G., Gillard, R. D., McCleverty, J. A., Eds.; Pergamon Press: Oxford, 1987; Vol. 2, pp 100. (c) Nugent, W. A.; Mayer, J. M. *Metal–Ligand Multiple Bonds*; Wiley-Interscience: New York, 1988.

($n = 4$ or 8 , H_2Me_n taa = tetra- or octa-methyldibenzotetraaza-[14]annulene) complexes with CO_2 .^{2g} These were the first reported reactions of a $Ti=NNR_2$ bond. Subsequently, Woo and Thorman described the synthesis of $Ti(NNR_2)(TTP)$ ($R = Me$ or Ph , $H_2TTP = meso$ -tetra-*p*-tolylporphyrin) and its reactions with *p*-chlorobenzaldehyde.^{2e} Very recently, Odom et al. reported the first crystallographically characterized terminal titanium hydrazido(2-), namely $Ti(NNMe_2)(dpma)$ -('Bu-bipy) ($dpma = N,N$ -di(pyrryl- α -methyl)-*N*-methylamine, 'Bu-bipy = 4,4'-di-*tert*-butyl-2,2'-bipyridine) which was used as a hydroamination catalyst.^{2a}

These terminal titanium hydrazido(2-) complexes were each prepared using different synthetic strategies. In this contribution, we report new and potentially general entry points to titanium hydrazido(2-) compounds (hereafter

referred to as "hydrazido"), together with a range of macrocycle-supported and related derivatives and a density functional theory (DFT) analysis of the bonding in terminal diphenylhydrazido compounds and their alkyl- and phenyl-imido analogues.⁹

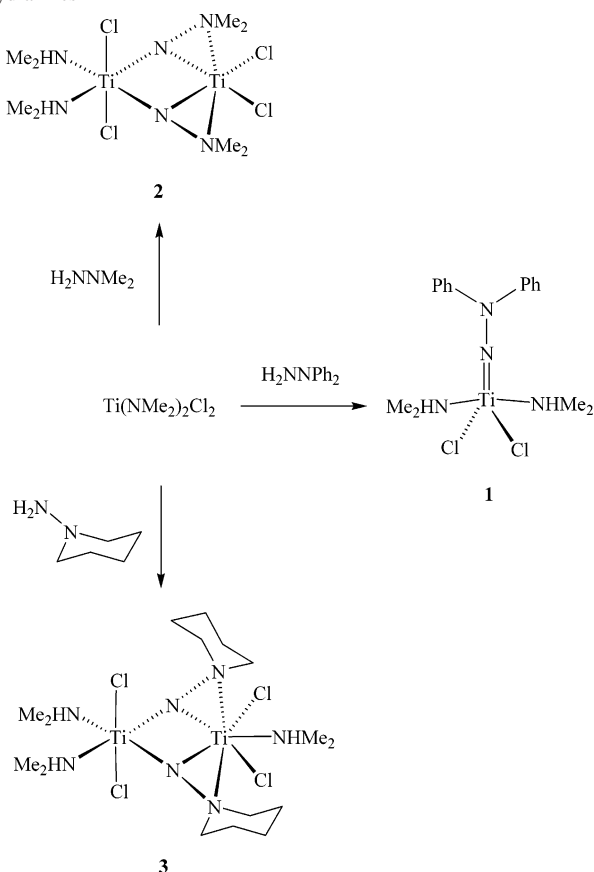
Results and Discussion

New Entry Points to Titanium Hydrazido Chemistry. $NHMe_2$ Adducts. We previously showed that reactions of primary amines RNH_2 ($R =$ alkyl or aryl) with the readily available $Ti(NMe_2)_2Cl_2$ ¹⁰ gave facile and high-yielding access to a family of monomeric titanium imido synthons of the type $Ti(NR)Cl_2(HNMe_2)_2$.¹¹ Such compounds have recently been useful in the MOCVD synthesis of TiN thin films,¹² the synthesis of calix[4]arene-supported terminal imido complexes,¹³ and the preparation of a library of highly active polymerization catalysts.¹⁴ We also showed^{11b} that certain complexes $Ti(NR)Cl_2(HNMe_2)_2$ could be converted to the bis- or tris-(pyridine) homologues $[Ti(NR)Cl_2(py)_m]_n$ ($m = 3, n = 1; m = n = 2$), themselves very useful precursors to new titanium imido chemistry.^{6a,f,15} We anticipated that 1,1-disubstituted hydrazines would react with $Ti(NMe_2)_2Cl_2$ in a fashion similar to primary amines and that it would be possible to use the resulting hydrazido complexes as new starting materials in titanium hydrazido chemistry. For initial studies in this area, three different commercially available 1,1-disubstituted hydrazines were chosen, namely, diphenylhydrazine, dimethylhydrazine, and *N*-aminopiperidine. The products of their reactions with $Ti(NMe_2)_2Cl_2$ are summarized in Scheme 1.

H_2NNPh_2 reacted smoothly at room temperature with $Ti(NMe_2)_2Cl_2$ to produce $Ti(NNPh_2)Cl_2(HNMe_2)_2$ (**1**) in a 91% isolated yield. Compound **1** was characterized by elemental analysis and NMR and IR spectroscopy. The ¹H NMR spectrum featured resonances corresponding to a $NNPh_2$ moiety and two coordinated $HNMe_2$ ligands by integration. The solid-state IR spectrum (Nujol mull) showed an absorption at 3254 cm^{-1} corresponding to a $\nu(N-H)$ stretch. This value lies within the range of frequencies ($3320\text{--}3273\text{ cm}^{-1}$) observed for the corresponding imido complexes $Ti(NR)Cl_2(NHMe_2)_2$ which exist as $N-H\cdots Cl$ hydrogen-bonded chains in the solid state.¹¹ Attempts to grow diffraction-quality crystals of **1** were unsuccessful. However, a cryoscopic molecular weight determination in benzene gave a

- (2) For selected recent references on early transition metal terminal hydrazido(2-) chemistry, see: (a) Li, Y.; Shi, Y.; Odom, A. L. *J. Am. Chem. Soc.* **2004**, *126*, 1794. (b) Yandulov, D. V.; Schrock, R. R. *Science* **2003**, *301*, 76. (c) Davies, S. C.; Hughes, D. L.; Konkol, M.; Richards, R. L.; Sanders, J. R.; Sobota, P. *J. Chem. Soc., Dalton Trans.* **2002**, 2811. (d) Greco, G. E.; Schrock, R. R. *Inorg. Chem.* **2001**, *40*, 3861. (e) Thorman, J. L.; Woo, L. K. *Inorg. Chem.* **2000**, *39*, 1301. (f) Redshaw, C.; Elsegood, M. R. *J. Inorg. Chem.* **2000**, *39*, 5164. (g) Blake, A. J.; McInnes, J. M.; Mountford, P.; Nikonov, G. I.; Swallow, D.; Watkin, D. J. *J. Chem. Soc., Dalton Trans.* **1999**, 379. (h) Dilworth, J. R.; Gibson, V. C.; Davies, N.; Redshaw, C.; White, A. P.; Williams, D. J. *J. Chem. Soc., Dalton Trans.* **1999**, 2695. (i) O'Donoghue, M. B.; Davis, W. M.; Schrock, R. R. *Inorg. Chem.* **1998**, *37*, 5149. (j) Davies, S. C.; Hughes, D. L.; Janas, Z.; Jerzykiewicz, L.; Richards, R. L.; Sanders, J. R.; Sobota, P. *Chem. Commun.* **1997**, 1261. (k) Green, M. L. H.; James, T. J.; Chernega, A. N. *J. Chem. Soc., Dalton Trans.* **1997**, 1719. (l) Green, M. L. H.; James, T. J.; Saunders, J. F.; Souter, J. *J. Chem. Soc., Dalton Trans.* **1997**, 1281.
- (3) For reviews of dinitrogen activation, see: (a) Gambarotta, S.; Scott, J. *Angew. Chem., Int. Ed.* **2004**, *43*, 5298. (b) Kozak, C. M.; Mountford, P. *Angew. Chem., Int. Ed.* **2004**, *43*, 1186. (c) Hidai, M.; Mizobe, Y. *Met. Ions Biol. Syst.* **2002**, *39*, 121. (d) Fryzuk, M. D.; Johnson, S. A. *Coord. Chem. Rev.* **2000**, *200*–202, 379. (e) Sellmann, D.; Sutter, J. *Acc. Chem. Res.* **1997**, *30*, 460. (f) Hidai, M. *Coord. Chem. Rev.* **1999**, *185*–186, 99. (g) Gambarotta, S. *J. Organomet. Chem.* **1995**, *500*, 117. (h) Hidai, M.; Mizobe, Y. *Chem. Rev.* **1995**, *95*, 1115.
- (4) Walsh, P. J.; Carney, M. J.; Bergman, R. G. *J. Am. Chem. Soc.* **1991**, *113*, 6343.
- (5) For selected examples of titanium hydrazido(1-) compounds, see: (a) Kim, S.-J.; Jung, I. N.; Yoo, B. R.; Cho, S.; Ko, J.; Kim, S. H.; Kang, S. O. *Organometallics* **2001**, *20*, 1501. (b) Park, J. T.; Yoon, S. C.; Bae, B.-J.; Seo, W. S.; Suh, I.-H.; Han, T. K.; Park, J. R. *Organometallics* **2000**, *19*, 1269. (c) Yoon, S. C.; Bae, B.-J.; Suh, I.-H.; Park, J. T. *Organometallics* **1999**, *18*, 2049. (d) Zippel, T.; Arndt, P.; Ohff, A.; Spannenberg, A.; Kempe, R.; Rosenthal, U. *Organometallics* **1998**, *17*, 4429. (e) Ohff, A.; Zippel, T.; Arndt, P.; Spannenberg, A.; Kempe, R.; Rosenthal, U. *Organometallics* **1998**, *17*, 1649. (f) Hill, J. E.; Fanwick, P. E.; Rothwell, I. P. *Inorg. Chem.* **1991**, *30*, 1143. (g) Hughes, D. L.; Jimenez-Tenorio, M.; Leigh, G. J.; Walker, D. G. *J. Chem. Soc., Dalton Trans.* **1989**, 2389. (h) Hughes, D. L.; Leigh, G. J.; Walker, D. G. *J. Chem. Soc., Dalton Trans.* **1989**, 1413. (i) Latham, I. A.; Leigh, G. J.; Huttner, G.; Jibril, I. *J. Chem. Soc., Dalton Trans.* **1986**, 385. (j) Dilworth, J. R.; Latham, I. A.; Leigh, G. J.; Huttner, G.; Jibril, I. *J. Chem. Soc., Chem. Commun.* **1983**, 1368.
- (6) For reviews featuring titanium imido chemistry, see: (a) Hazari, N.; Mountford, P. *Acc. Chem. Res.*, in press (ar030244z). (b) Odom, A. L. *Dalton Trans.* **2005**, 225. (c) Bolton, P. D.; Mountford, P. *Adv. Synth. Catal.* **2005**, *347*, 355. (d) Mountford, P. In *Perspectives in Organometallic Chemistry*; Screttas, C. G., Steele, B. R., Eds.; Royal Society of Chemistry: Cambridge, 2003. (e) Gade, L. H.; Mountford, P. *Coord. Chem. Rev.* **2001**, *216*–217, 65. (f) Mountford, P. *Chem. Commun.* **1997**, 2127. (g) Wigley, D. E. *Prog. Inorg. Chem.* **1994**, *42*, 239.
- (7) (a) Hughes, D. L.; Latham, I. A.; Leigh, G. J. *J. Chem. Soc., Dalton Trans.* **1986**, 393. (b) Latham, I. A.; Leigh, G. J. *J. Chem. Soc., Dalton Trans.* **1986**, 399.
- (8) Wiberg, N.; Haering, H. W.; Huttner, G.; Friedrich, P. *Chem. Ber.* **1978**, *111*, 2708.

- (9) Although for the sake of convenience the titanium-imido and -hydrazido linkages herein are drawn as "Ti=NR", it is most appropriate to consider them as metal-ligand triple bonds.
- (10) Froneman, M.; Cheney, D. L.; Modro, T. A. *Phosphorus, Sulfur Silicon Relat. Elem.* **1990**, 47.
- (11) (a) Adams, N.; Cowley, A. R.; Dubberley, S. R.; Sealey, A. J.; Skinner, M. E. G.; Mountford, P. *Chem. Commun.* **2001**, 2738. (b) Adams, N.; Bigmore, H. R.; Blundell, T. L.; Boyd, C. L.; Dubberley, S. R.; Sealey, A. J.; Cowley, A. R.; Skinner, M. E. G.; Mountford, P. *Inorg. Chem.* **2005**, *44*, 2882.
- (12) Carmalt, C. J.; Newport, A.; Parkin, I. P.; Mountford, P.; Sealey, A. J.; Dubberley, S. R. *J. Mater. Chem.* **2003**, *13*, 84.
- (13) Dubberley, S. R.; Friedrich, A.; Willman, D. A.; Mountford, P.; Radius, U. *Chem.—Eur. J.* **2003**, *9*, 3634.
- (14) Adams, N.; Arts, H. J.; Bolton, P. D.; Cowell, D.; Dubberley, S. R.; Friederichs, N.; Grant, C. M.; Kranenburg, M.; Sealey, A. J.; Wang, B.; Wilson, P. J.; Cowley, A. R.; Mountford, P.; Schröder, M. *Chem. Commun.* **2004**, 434.

Scheme 1. Reactions of $\text{Ti}(\text{NMe}_2)_2\text{Cl}_2$ with 1,1-Disubstituted Hydrazines

value of 417 g mol^{-1} which is close to the expected value (391.1 g mol^{-1}) for the monomeric species depicted in Scheme 1. The approximately trigonal-pyramidal geometry proposed is based on that found crystallographically for monomeric imido $\text{Ti}(\text{NR})\text{Cl}_2(\text{NHMe}_2)_2$ ($\text{R} = \text{iPr, Ph, C}_6\text{F}_5, \text{C}_6\text{Cl}_4\text{H, 2-C}_6\text{H}_4\text{CF}_3, \text{and 2-C}_6\text{H}_4\text{tBu}$) compounds.¹¹ All structurally characterized compounds of the type “ $\text{M}(\text{NR})\text{-Cl}_2(\text{NHMe}_2)_2$ ” ($\text{M} = \text{Ti}^{\text{IV}}$ or V^{IV}) reported to date have possessed monomeric structures.

The reaction of 1 equiv of either dimethylhydrazine or *N*-aminopiperidine with $\text{Ti}(\text{NMe}_2)_2\text{Cl}_2$ in benzene resulted in the formation of dinuclear hydrazido-bridged $\text{Ti}_2(\mu-\eta^2, \eta^1\text{-NNMe}_2)_2\text{Cl}_4(\text{HNMe}_2)_2$ (**2**) or $\text{Ti}_2\{\mu-\eta^2, \eta^1\text{-NN}(\text{CH}_2)_5\}_2\text{Cl}_4(\text{HNMe}_2)_3$ (**3**) (Scheme 1). The solubility of both complexes is substantially lower than that of **1**. Their dimeric nature was confirmed by X-ray diffraction (vide infra), and the ^1H NMR spectrum of **2** showed resonances for a NNMe_2 ligand and one NHMe_2 ligand (per hydrazido moiety), consistent with the proposed structures. Both compounds show $\nu(\text{N-H})$ bands in the expected region for $\text{N-H}\cdots\text{Cl}$ hydrogen bonding¹¹ in their IR spectra, and this is consistent with the solid-state structures as discussed later. It is interesting to

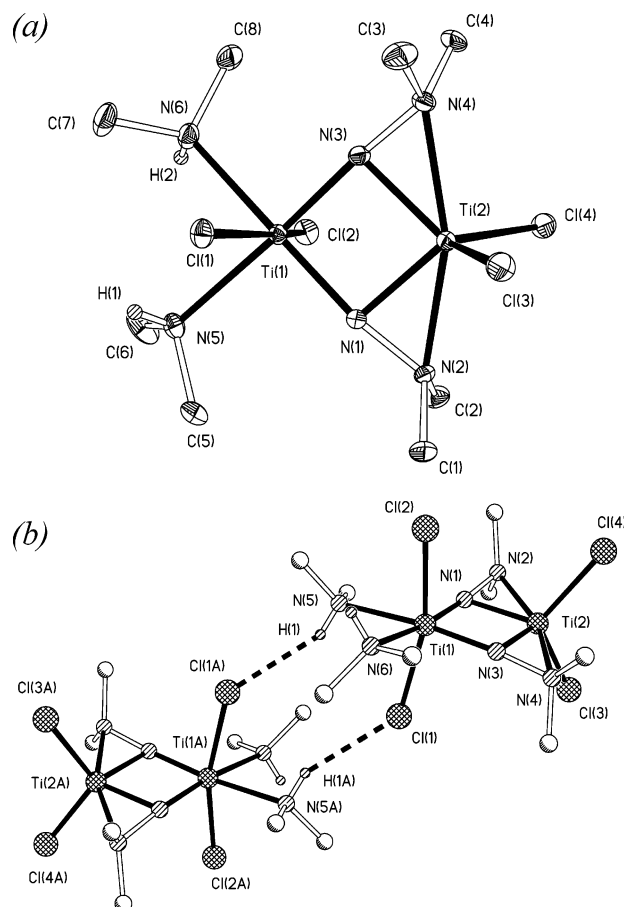


Figure 1. (a) Displacement ellipsoid plot (30% probability) of $\text{Ti}_2(\mu-\eta^2, \eta^1\text{-NNMe}_2)_2\text{Cl}_4(\text{HNMe}_2)_2$ (**2**). Carbon-bound H atoms are omitted for clarity, and the other H atoms are shown as spheres of arbitrary radius. (b) Ball and stick view of the $\text{N-H}\cdots\text{Cl}$ hydrogen bonded pairs of **2**. Atoms carrying the suffix A are related their counterparts by the operator $[1 - x, 1 - y, -z]$.

note the presence of the third NHMe_2 coordinated to one of the titanium centers in **3**. This “extra” coordinated amine (in contrast to the bis(dimethylamine) homologue **2**) could not be removed under vacuum. Odom has recently reported the bis(hydrazido-bridged) dititanium compound $\text{Ti}_2(\mu-\eta^2, \eta^1\text{-NNMe}_2)_2(\text{dpma})_2$ containing one seven-coordinate titanium center and one six-coordinate one.^{2a} Overall, the reactions of $\text{Ti}(\text{NMe}_2)_2\text{Cl}_2$ with 1,1-disubstituted hydrazines suggest that terminal hydrazido compounds (e.g., **1**) are accessible provided that sufficient steric bulk is available to prevent the formation of hydrazido-bridged dimers.

The molecular and supramolecular structures of **2** and **3** are shown in Figures 1 and 2, respectively, and selected distances and angles are given in Tables 1 and 2. Both compounds feature $\text{Ti}_2(\mu-\eta^2, \eta^1\text{-NNR}_2)_2$ units with the titanium coordination spheres being completed by Cl and NHMe_2 ligands. In **2**, the Ti-Cl bonds lie approximately perpendicular to the plane containing the $\text{Ti}_2(\mu\text{-NN})_2$ moiety, whereas in **3**, two of the Cl ligands lie within this plane. Atom Ti(1) in each case has an approximately octahedral geometry, being coordinated to two Cl ligands, two NHMe_2 ligands, and one nitrogen of each of the two bridging hydrazido ligands. Ti(2) in **2** has a highly distorted octahedral geometry, whereas in **3**, Ti(2) has a distorted pentagonal

(15) (a) Nielson, A. J.; Glenny, M. W.; Rickard, C. E. *J. Chem. Soc., Dalton Trans.* **2001**, 232. (b) Li, Y.; Banerjee, S.; Odom, A. L. *Organometallics* **2005**, *24*, 3272. (c) Male, N. A. H.; Skinner, M. E. G.; Bylikin, S. Y.; Wilson, P. J.; Mountford, P.; Schröder, M. *Inorg. Chem.* **2000**, *39*, 5483.

(16) Lorber, C.; Choukroun, R.; Donnadieu, B. *Inorg. Chem.* **2002**, *41*, 4217.

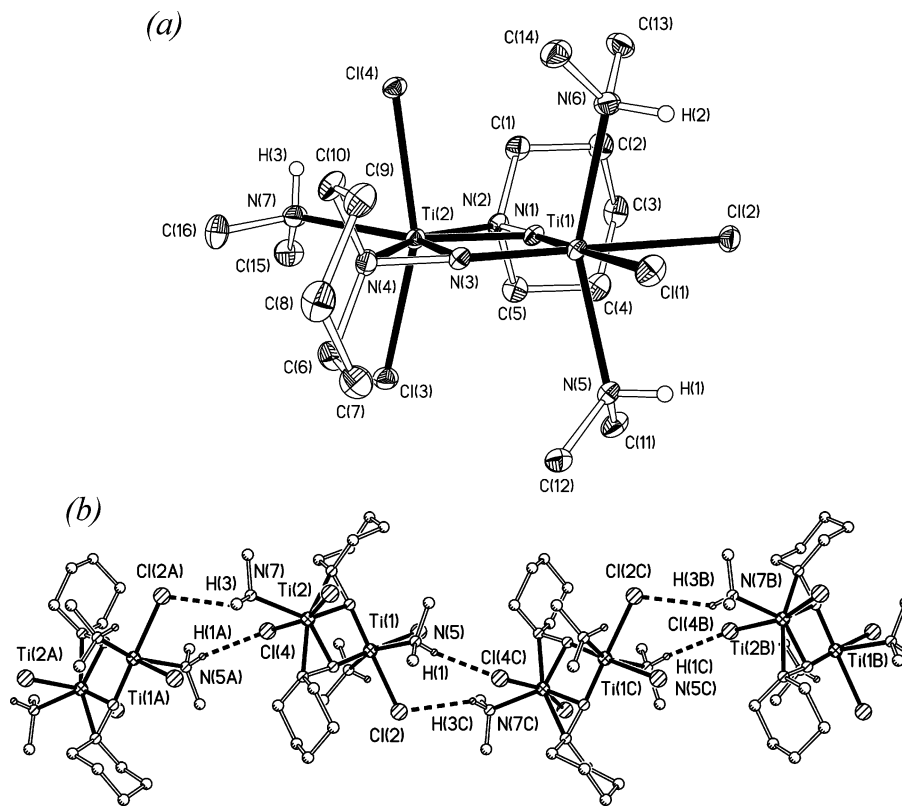


Figure 2. (a) Displacement ellipsoid plot (30% probability) of $\text{Ti}_2\{\mu\text{-}\eta^2, \eta^1\text{-NN}(\text{CH}_2)_5\}_2\text{Cl}_4(\text{HNMe}_2)_3$ (**3**). Benzene molecules of crystallization and carbon-bound H atoms are omitted for clarity, and all other H atoms are shown as spheres of arbitrary radius. (b) Ball and stick view of a portion of the N–H \cdots Cl hydrogen-bonded chain of **3**. Atoms carrying the suffixes A, B, and C are related their counterparts by the operators $[1 - x, y - 1/2, 1/2 - z]$, $[x, y + 1, z]$, and $[1 - x, y + 1/2, 1/2 - z]$, respectively.

Table 1. Selected Bond Lengths (Å) and Angles (deg) for $\text{Ti}_2\{\mu\text{-}\eta^2, \eta^1\text{-NNMe}_2\}_2\text{Cl}_4(\text{HNMe}_2)_2$ (**2**)^a

Ti(1)–Cl(1)	2.4068(7)	Ti(2)–Cl(3)	2.2972(7)
Ti(1)–Cl(2)	2.3875(7)	Ti(2)–Cl(4)	2.2935(7)
Ti(1)–N(1)	1.8582(19)	Ti(2)–N(1)	1.922(2)
Ti(1)–N(3)	1.858(2)	Ti(2)–N(3)	1.918(2)
Ti(1)–N(5)	2.296(2)	Ti(2)–N(2)	2.198(2)
Ti(1)–N(6)	2.300(2)	Ti(2)–N(4)	2.185(2)
N(1)–N(2)	1.391(3)	N(3)–N(4)	1.386(3)
H(1) \cdots Cl(1A)	2.67		
Cl(1)–Ti(1)–Cl(2)	164.54(3)	Cl(3)–Ti(2)–Cl(4)	116.37(3)
N(1)–Ti(1)–N(3)	88.06(8)	N(1)–Ti(2)–N(3)	84.55(8)
N(5)–Ti(1)–N(6)	85.56(8)	N(2)–Ti(2)–N(4)	161.16(8)
Ti(1)–N(1)–Ti(2)	93.63(9)	Ti(1)–N(3)–Ti(2)	93.75(9)
Ti(1)–N(1)–N(2)	166.20(17)	Ti(1)–N(3)–N(4)	169.78(17)
N(5)–H(1) \cdots Cl(1A)	152		

^a Atoms carrying the suffix A are related their counterparts by the operator $[1 - x, 1 - y, -z]$.

bipyramidal geometry. The small N(1)–Ti(2)–N(3) or N(2)–Ti(1)–N(4) angles are responsible for the major deviations from the ideal geometries. Molecules of **2** exist as N–H \cdots Cl hydrogen-bonded dimers in the solid state with one NHMe₂ and one Cl ligand of each Ti(1) center participating in these interactions. The other NHMe₂ and Cl ligands are not involved in intermolecular contacts. Molecules of **3** form N–H \cdots Cl hydrogen-bonded chains because of the participation of the Ti(2)-bound NHMe₂ ligand. These chains propagate along the crystallographic *b* axis. Again, only one NHMe₂ and one Cl ligand of Ti(1) are involved in hydrogen bonding and only one of the Cl ligands bound to Ti(2). The distances and angles associated with the

Table 2. Selected Bond Lengths (Å) and Angles (deg) for $\text{Ti}_2\{\mu\text{-}\eta^2, \eta^1\text{-NN}(\text{CH}_2)_5\}_2\text{Cl}_4(\text{HNMe}_2)_3$ (**3**)^a

Ti(1)–Cl(1)	2.4907(7)	Ti(2)–Cl(3)	2.3543(7)
Ti(1)–Cl(2)	2.4956(7)	Ti(2)–Cl(4)	2.3984(7)
Ti(1)–N(1)	1.8574(19)	Ti(2)–N(1)	1.947(2)
Ti(1)–N(3)	1.848(2)	Ti(2)–N(3)	1.966(2)
Ti(1)–N(5)	2.220(2)	Ti(2)–N(2)	2.210(2)
Ti(1)–N(6)	2.262(2)	Ti(2)–N(4)	2.244(2)
N(1)–N(2)	1.398(3)	Ti(2)–N(7)	2.311(2)
N(3)–N(4)	1.397(3)	H(3) \cdots Cl(2A)	2.85
H(1A) \cdots Cl(4)	2.56		
Cl(1)–Ti(1)–Cl(2)	85.68(3)	Cl(3)–Ti(2)–Cl(4)	159.19(3)
N(1)–Ti(1)–N(3)	88.73(9)	N(1)–Ti(2)–N(3)	82.92(8)
N(5)–Ti(1)–N(6)	153.67(9)	N(2)–Ti(2)–N(4)	159.60(8)
Ti(1)–N(1)–Ti(2)	94.32(9)	Cl(3)–Ti(2)–N(7)	82.48(6)
Ti(1)–N(1)–N(2)	175.15(16)	Cl(4)–Ti(2)–N(7)	77.03(6)
Ti(1)–N(3)–Ti(2)	93.96(9)	Ti(1)–N(3)–N(4)	175.64(17)
N(7)–H(3) \cdots Cl(2A)	143	N(5A)–H(1A) \cdots Cl(4)	147

^a Atoms carrying the suffixes A, B, and C are related their counterparts by the operators $[1 - x, y - 1/2, 1/2 - z]$, $[x, y + 1, z]$, and $[1 - x, y + 1/2, 1/2 - z]$, respectively.

N–H \cdots Cl hydrogen bonds are comparable to those found in the supramolecular structures of $\text{Ti}(\text{NR})\text{Cl}_2(\text{NHMe}_2)_2$ ($\text{R} = \text{}^i\text{Pr}$, Ph, $\text{C}_6\text{Cl}_4\text{H}$, $2\text{-C}_6\text{H}_4\text{CF}_3$, and $2\text{-C}_6\text{H}_4\text{}^t\text{Bu}$)^{11b} and transition metal chloride compounds in general.¹⁷

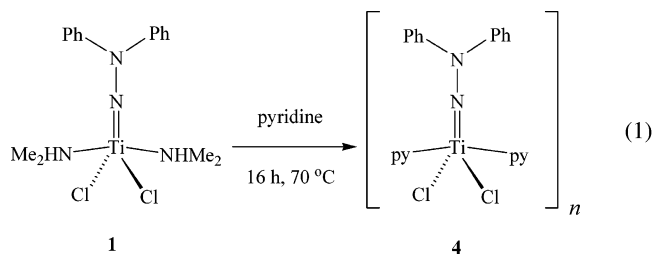
The point of main interest in **2** and **3** are the $\text{Ti}_2(\mu\text{-}\eta^2, \eta^1\text{-NNR}_2)_2$ moieties. The Ti(1)–N distances are equivalent within error for the two compounds while the Ti(2)–N distances differ slightly between **2** and **3**, presumably because

(17) Aullón, G.; Bellamy, D.; Brammer, L.; Bruton, E. A.; Orpen, A. G. *Chem. Commun.* **1998**, 653.

of the different hydrazide R-substituents and Ti(2) coordination numbers. In each compound, the Ti(1)–N–NR₂ linkages are approximately linear (av Ti(1)–N–NR₂ = 168.0° and 175.4° for **2** and **3**, respectively) with an average N–N distance of 1.393 Å which is approaching that of a single N–N bond distance (1.451 ± 0.005 Å) for compounds of the type R₂N–NR₂.¹⁸ The Ti(1)–N(1) and Ti(1)–N(3) distances (av 1.855 Å) are somewhat shorter than those to Ti(2) for these atoms (av 1.938 Å). The Ti(2)–N(2) and Ti(2)–N(4) distances are longest of all (av 2.209 Å) in the Ti₂(μ-η²,η¹-NNR₂)₂ moieties, reflecting the neutral, sp³-hybridized nature of the N(2) and N(4) atoms.

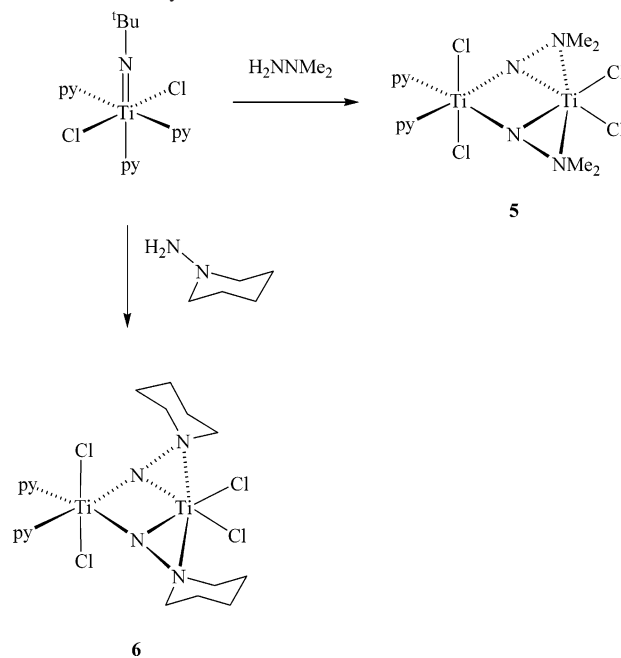
Compounds containing a structurally characterized M(μ-η²,η¹-NNR₂)M unit are not common, and only five have been reported to date (av N–N distance 1.400 Å, range 1.383–1.424 Å).¹⁹ Only one has two μ-η²,η¹-bridging ligands, this being Odom's Ti₂(μ-η²,η¹-NNMe₂)₂(dpma)₂.^{2a} The only other examples from Group 4 contain one μ-η²,η¹-coordinated ligand and one that is μ-η¹,η¹-coordinated; these are CpTiCl(μ-η²,η¹-NNPh₂)(μ-η¹,η¹-NNPh₂)TiCpCl^{7a} and Cp₂Zr(μ-η²,η¹-NNPh₂)(μ-η²,η¹-NNPh₂)ZrCp₂.⁴ The different coordination modes in the latter two compounds may reflect the increased steric demands of bridging 1,1-diphenylhydrazido ligands as opposed to the less sterically demanding ones present in Ti₂(μ-η²,η¹-NNMe₂)₂(dpma)₂, **2** and **3** (and also **5**, vide infra).

Pyridine Adducts. As mentioned, the pyridine-supported compound Ti(N^tBu)Cl₂(py)₃²⁰ allows general access to new titanium *tert*-butyl imido compounds through chloride or pyridine ligand metathesis. In certain cases, the use of this pyridine adduct instead of the bis(dimethylamino) homologue Ti(N^tBu)Cl₂(NHMe₂)₂¹¹ is preferred (for example when other reagents present could react with the amino N–H bond or if a good Lewis base such as pyridine is required for stabilizing the target product). Furthermore, Ti(N^tBu)Cl₂(py)₃ undergoes *tert*-butyl imide/amine exchange reactions (N^tBuNH₂ elimination) with anilines^{15a,20} or other amines^{15b,c} to give new monomeric imido compounds or their halide-bridged terminal imido analogues Ti₂(NR)₂Cl₂(μ-Cl)₂(py)₄, both also useful reagents in titanium imido chemistry. In a previous paper,^{2e} we showed that the macrocycle-supported compound Ti(N^tBu)(Me_ntaa) reacted with H₂NNPh₂ to give the corresponding terminal hydrazido derivatives Ti(NNPh₂)(Me_ntaa). It was of interest, therefore, to explore the reactions of Ti(N^tBu)Cl₂(py)₃ with 1,1-disubstituted hydrazines.



Although H₂NNMe₂ and N-aminopiperidine undergo clean *tert*-butyl imide exchange reactions with Ti(N^tBu)Cl₂(py)₃ (vide infra and Scheme 2), the corresponding reaction with

Scheme 2. Selected Reactions of Ti(N^tBu)Cl₂(py)₃ with 1,1-Disubstituted Hydrazines



H₂NNPh₂ (1 equiv) produced a complex mixture of products (including the expected ^tBuNH₂ side product). Similarly, reaction of Ti(NNPh₂)Cl₂(NHMe₂)₂ (**1**) with several equivalents of pyridine in benzene gave a mixture of products which appeared to contain coordinated pyridine and NHMe₂. However, heating (70 °C) a solution of **1** in neat pyridine for 16 h gave clean conversion to [Ti(NNPh₂)Cl₂(py)₂]_n (**4**, eq 1). An analogous method was used previously^{11b} for the conversion of the imido compounds Ti(NR)Cl₂(NHMe₂)₂ (R = ^tBu, C₆F₅, or 4-C₆H₄Cl) to the corresponding pyridine adducts Ti₂(N^tBu)₂Cl₂(μ-Cl)₂(py)₄ or Ti(NR)Cl₂(py)₃ (R = C₆F₅ or 4-C₆H₄Cl). The loss of pyridine (that nominally coordinated trans to the Ti=NR bond) from compounds of the type Ti(NR)Cl₂(py)₃ under vacuum is well-known^{15a,20} and has been attributed to the strong trans influence of the imido ligand.

Compound **4** was characterized by spectroscopic methods and elemental analysis, but unfortunately, it was too insoluble to allow an accurate solution molecular weight determination. However, we consider it to be very likely (at least in the solid state) that **4** exists as a chloride-bridged *terminal* hydrazido dimer Ti₂(NNPh₂)₂Cl₂(μ-Cl)₂(py)₄ of the type found to date in the solid state for all the related structurally characterized^{11b,15a,b,21} bis(pyridine) titanium imido compounds “Ti(NR)Cl₂(py)₂” (note that Odom has found that “Ti(NSiPh₃)Cl₂(py)₂” is a chloride-bridged dimer in the solid state but monomeric in solution^{15b}). The following indirect evidence points to a terminal hydrazido structure for **4**. First,

(18) Gordon, A. J.; Ford, R. A. *The Chemist's Companion*; Wiley-Interscience: New York, 1972; p 107.

(19) For the Cambridge Structural Database, see: (a) Allen, F. H.; Kennard, O. *Chem. Des. Autom. News* **1993**, *8*, 1 & 31. (b) Fletcher, D. A.; McMeeking, R. F.; Parkin, D. J. *Chem. Inf. Comput. Sci.* **1996**, *36*, 746.

(20) Blake, A. J.; Collier, P. E.; Dunn, S. C.; Li, W.-S.; Mountford, P.; Shishkin, O. V. *J. Chem. Soc., Dalton Trans.* **1997**, 1549.

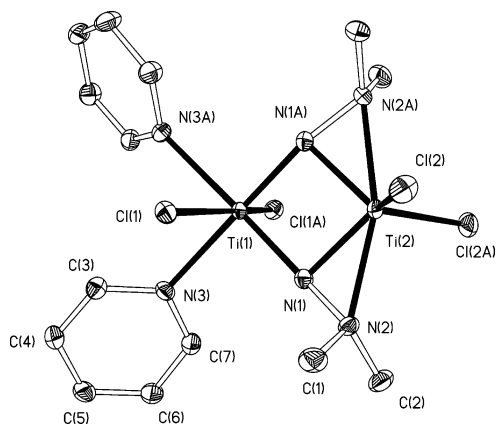


Figure 3. Displacement ellipsoid plot (30% probability) of $\text{Ti}_2(\mu\text{-}\eta^2, \eta^1\text{-NNMe}_2)_2\text{Cl}_4(\text{py})_2$ (**5**). H atoms are omitted for clarity. Atoms carrying the suffix A are related their counterparts by the operator $[1 - x, y, 1/2 - z]$.

Table 3. Selected Bond Lengths (Å) and Angles (deg) for $\text{Ti}_2(\mu\text{-}\eta^2, \eta^1\text{-NNMe}_2)_2\text{Cl}_4(\text{py})_2$ (**5**)

Ti(1)–Cl(1)	2.3950(6)	Ti(2)–Cl(2)	2.2889(8)
Ti(1)–N(1)	1.867(2)	Ti(2)–N(1)	1.920(2)
Ti(1)–N(3)	2.277(2)	Ti(2)–N(2)	2.206(2)
N(1)–N(2)	1.379(3)		
Cl(1)–Ti(1)–Cl(1A)	164.10(4)	Cl(2)–Ti(2)–Cl(2A)	117.27(5)
N(1)–Ti(1)–N(1A)	87.91(13)	N(1)–Ti(2)–N(1A)	84.94(13)
N(3)–Ti(1)–N(3A)	86.59(12)	N(2)–Ti(2)–N(2A)	159.97(12)
Ti(1)–N(1)–Ti(2)	93.58(10)	Ti(1)–N(1)–N(2)	165.12(18)

the EI mass spectra of the structurally characterized dimers **2** and **3** (Scheme 1) and of the corresponding dimeric pyridine compounds $\text{Ti}_2(\mu\text{-}\eta^2, \eta^1\text{-NNR}_2)_2\text{Cl}_4(\text{py})_2$ ($\text{R} = \text{Me}$ (**5**), $\text{R}_2 = (\text{CH}_2)_5$ (**6**), vide infra and Scheme 2) feature well-defined dimeric fragment ions $[\text{Ti}_2(\text{NNR}_2)_2]^+$ with the correct m/z ratio and isotope patterns, whereas **4** shows a well-defined envelope only for the monomeric $[\text{TiNNPh}]^+$ fragment. Furthermore, while **1** (monomeric) and **4** react readily with a range of *fac*- N_3 donor ligands to form six-coordinate terminal hydrazido $\text{Ti}(\text{NNPh}_2)\text{Cl}_2(\text{fac}\text{-N}_3)$ compounds (vide infra), the dimeric compounds **2** and **3** and **5** and **6** do not react at all (consistent with them possessing unreactive $\text{Ti}_2(\mu\text{-}\eta^2, \eta^1\text{-NNR}_2)_2$ cores).

As mentioned, $\text{Ti}(\text{N}^t\text{Bu})\text{Cl}_2(\text{py})_3$ reacts smoothly with $\text{H}_2\text{-NNMe}_2$ or *N*-aminopiperidine to yield dimeric pyridine $\text{Ti}_2(\mu\text{-}\eta^2, \eta^1\text{-NNR}_2)_2\text{Cl}_4(\text{py})_2$ ($\text{R} = \text{Me}$ (**5**), $\text{R}_2 = (\text{CH}_2)_5$ (**6**)) compounds. Compound **5** features resonances for NNMe_2 and coordinated pyridine ligands (1:1 ratio) and has been crystallographically characterized. Compound **6** was too insoluble to obtain NMR data (cf. **3**) but on the basis of elemental analysis appears to contain two pyridine ligands as indicated in Scheme 2. The molecular structure of **5** is shown in Figure 3, and selected bond distances and angles are given in Table 3. Molecules of **5** lie on crystallographic 2-fold rotation axes which pass through the $\text{Ti}(1)\cdots\text{Ti}(2)$ vector. The molecular structure of **5** is very similar to that of $\text{Ti}_2(\mu\text{-}\eta^2, \eta^1\text{-NNMe}_2)_2\text{Cl}_4(\text{NHMe}_2)_2$ (**2**) with the NHMe_2 ligands formally replaced by pyridines (the $\text{Ti}(1)\text{-N}(3)$ distance is typical for a Ti-bound pyridine ligand¹⁹). The distances and angles associated with the $\text{Ti}_2(\mu\text{-}\eta^2, \eta^1\text{-NNMe}_2)_2$ cores in the two compounds are equivalent with experimental

error. Unlike **2** and **3**, molecules of **5** show no significant intermolecular interactions.

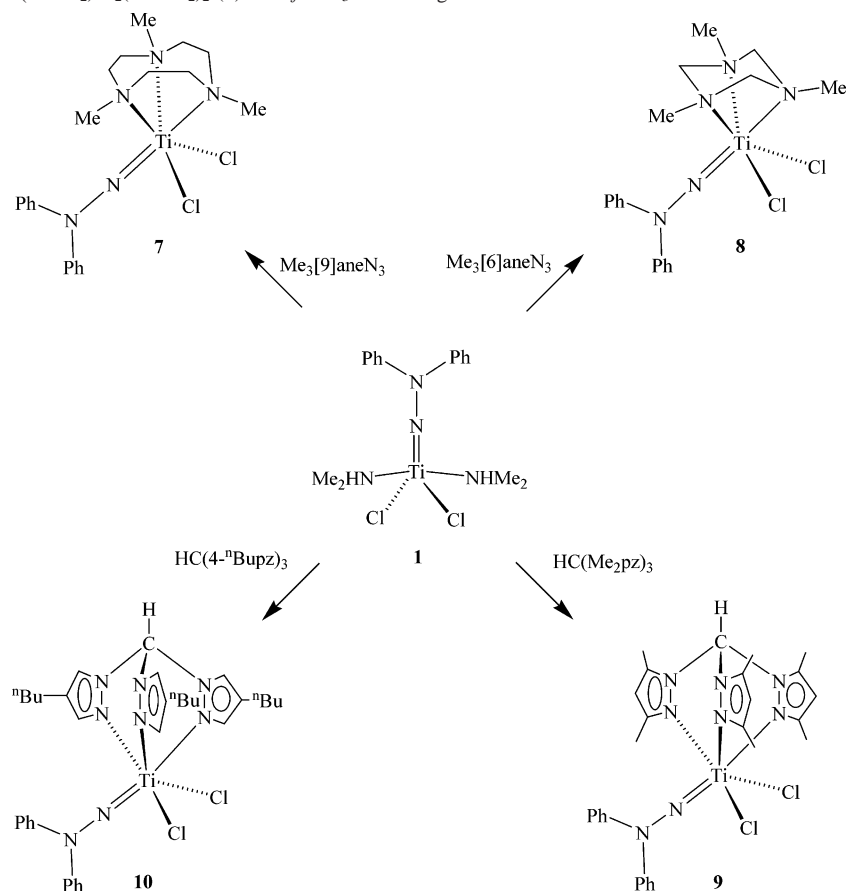
Titanium η^1 -Hydrazido Complexes with *fac*- N_3 Donor Ligands. We have recently been developing the stoichiometric and catalytic chemistry of titanium imido compounds supported by tridentate *fac*- N_3 donor ligands.^{14,15c,22} The compounds of the type $\text{Ti}(\text{NR})\text{X}_2(\text{fac}\text{-N}_3)$ ($\text{R} = \text{alkyl}$ or aryl , $\text{X} = \text{Cl}$ or alkyl) are isolobal analogues of metallocenes Cp_2MX_2 (for $\text{X} = \text{Cl}$) and are accessible via the reaction of the imido synthons $\text{Ti}(\text{NR})\text{Cl}_2(\text{py})_3$ or $\text{Ti}(\text{NR})\text{Cl}_2(\text{NHMe}_2)_2$ with the appropriate *fac*- N_3 donor ligand. It was therefore of interest to explore the parallel reactions of representative *fac*- N_3 donor ligands with compounds $\text{Ti}(\text{NNPh}_2)\text{Cl}_2(\text{NHMe}_2)_2$ (**1**) and $\text{Ti}(\text{NNPh}_2)\text{Cl}_2(\text{NHMe}_2)_2$ (**4**) to establish a framework for future studies.

The reactions of **1** with the *fac*- N_3 donor ligands $\text{Me}_3[9]\text{-aneN}_3$ (trimethyl-1,4,7-triazacyclononane), $\text{Me}_3[6]\text{aneN}_3$ (trimethyl-1,3,5-triazacyclohexane), $\text{HC}(\text{Me}_2\text{pz})_3$ (tris(3,5-dimethylpyrazolyl)methane), and $\text{HC}(\text{Bupz})_3$ (tris(4-*n*-butylpyrazolyl)methane) are summarized in Scheme 3. The reaction with 1 equiv of the appropriate *fac*- N_3 donor ligand proceeded smoothly in a 68–81% yield in benzene to give $\text{Ti}(\text{NNPh}_2)\text{Cl}_2(\text{Me}_3[9]\text{aneN}_3)$ (**7**), $\text{Ti}(\text{NNPh}_2)\text{Cl}_2(\text{Me}_3[6]\text{aneN}_3)$ (**8**), $\text{Ti}(\text{NNPh}_2)\text{Cl}_2\{\text{HC}(\text{Me}_2\text{pz})_3\}$ (**9**), and $\text{Ti}(\text{NNPh}_2)\text{Cl}_2\{\text{HC}(\text{Bupz})_3\}$ (**10**) as analytically and spectroscopically pure solids. They are proposed to be six-coordinate monomeric η^1 -hydrazido compounds on the basis of the available data and the X-ray crystal structure of **9** (vide infra). Reaction of **4** on the NMR-tube scale with $\text{Me}_3[9]\text{aneN}_3$, $\text{Me}_3[6]\text{aneN}_3$, $\text{HC}(\text{Me}_2\text{pz})_3$, and $\text{HC}(\text{Bupz})_3$ also resulted in the quantitative formation of complexes **7–10**, demonstrating that **4** can also be used as a titanium hydrazido synthon. In contrast, neither **2** nor **3** react with these *fac*- N_3 donor ligands, implying that the $\mu\text{-}\eta^2, \eta^1$ -hydrazido bridges in **2** and **3** are not readily cleaved.

The ^1H NMR spectra of compounds **7–10** all feature characteristic resonances in the region of 6.8–7.5 ppm corresponding to the diphenylhydrazido ligand. The resonances for the coordinated *fac*- N_3 donor ligands were as expected on the basis of previous studies and were consistent with the C_s symmetry proposed in Scheme 3 (see Experimental Section for further details). As was found in the corresponding imido compounds $\text{Ti}(\text{NR})(\text{Me}_3[6]\text{aneN}_3)\text{X}_2$ ($\text{X} = \text{Cl}$, $\text{R} = \text{Bu}$ or 2,6- $\text{C}_6\text{H}_3\text{Pr}_2$; $\text{X} = \text{CH}_2\text{Ph}$, $\text{R} = \text{Bu}$),^{22d} the $\text{Me}_3[6]\text{aneN}_3$ ligand in **8** undergoes a slow fluxional process at room temperature interpreted as a trigonal twist rearrangement that exchanges the macrocyclic ring *N*-methylene groups and each of the “up” and each of the “down” (with respect to the titanium center) methylene H atoms (no exchange is seen between any of the “up” with any of the

(21) Hazari, N.; Cowley, A. R.; Mountford, P. *Acta Crystallogr.* **2004**, *E60*, m1844.

(22) (a) Bolton, P. D.; Clot, E.; Cowley, A. R.; Mountford, P. *Chem. Commun.* **2005**, 3313. (b) Lawrence, S. C.; Skinner, M. E. G.; Green, J. C.; Mountford, P. *Chem. Commun.* **2001**, 705. (c) Gardner, J. D.; Robson, D. A.; Rees, L. H.; Mountford, P. *Inorg. Chem.* **2001**, *40*, 820. (d) Wilson, P. J.; Blake, A. J.; Mountford, P.; Schröder, M. *J. Organomet. Chem.* **2000**, *600*, 71. (e) Wilson, P. J.; Blake, A. J.; Mountford, P.; Schröder, M. *Chem. Commun.* **1998**, 1007. (f) Dunn, S. C.; Mountford, P.; Shishkin, O. V. *Inorg. Chem.* **1996**, *35*, 1006.

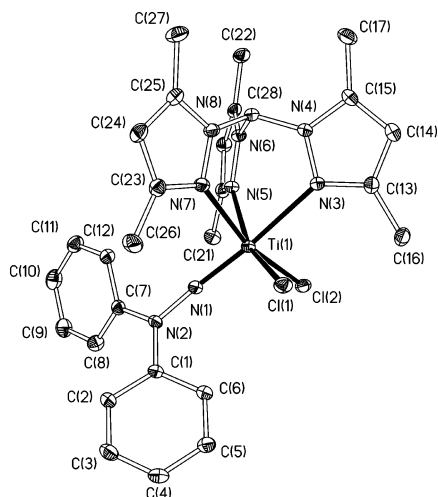
Scheme 3. Reactions of $\text{Ti}(\text{NNPh}_2)\text{Cl}_2(\text{NHMe}_2)_2$ (**1**) with *fac*- N_3 Donor Ligands

“down” methylene hydrogens showing (just as for the imido analogues) that this is an in-place rather than dissociative process). The fluxional process for **8** was readily confirmed by spin saturation transfer (SST) experiments between the *cis* and *trans* (with respect to $\text{Ti}=\text{NNPh}_2$) macrocycle *N*-Me groups at 298 K, and the process is frozen out by 260 K (in CD_2Cl_2). The rate constants for exchange between the ring methyl groups were measured by SST at seven temperatures

in the range of 283–307 K, and an Eyring analysis²³ gave the activation parameters $\Delta H^\ddagger = 54.9 \pm 1.7 \text{ kJ mol}^{-1}$ and $\Delta S^\ddagger = -42 \pm 6 \text{ J mol}^{-1} \text{ K}^{-1}$ ($\Delta G^\ddagger_{298} = 67.3 \pm 2.4 \text{ kJ mol}^{-1}$). These values are comparable with those found previously for the imido systems $\text{Ti}(\text{NR})(\text{Me}_3[6]\text{aneN}_3)\text{X}_2$ ($\Delta H^\ddagger = 46.7 \pm 3.3$ to $66.2 \pm 1.3 \text{ kJ mol}^{-1}$, $\Delta S^\ddagger = 11 \pm 5$ to $-40 \pm 13 \text{ J mol}^{-1} \text{ K}^{-1}$).^{22d}

The molecular structure of $\text{Ti}(\text{NNPh}_2)\text{Cl}_2\{\text{HC}(\text{Me}_2\text{pz})_3\}$ (**9**) is shown in Figure 4, and selected bond lengths and angles are given in Table 4. Molecules of **9** contain an approximately octahedral Ti center ligated by a *fac*-coordinated $\text{HC}(\text{Me}_2\text{pz})_3$ group, two *cis*-chloride ligands, and a terminal linear diphenylhydrazido ligand ($\text{Ti}(1)-\text{N}(1)-\text{N}(2) = 176.03(16)^\circ$). Compound **9** is the second structurally characterized terminal hydrazido complex of titanium (the first being Odom’s recent dimethylhydrazide $\text{Ti}(\text{NNMe}_2)(\text{dpma})(\text{tBu-bipy})$).^{2a} Only one other terminal hydrazido compound of Group 4 is known, namely, $\text{Cp}_2\text{Zr}(\text{NNPh}_2)(4\text{-NC}_5\text{H}_4\text{NMe}_2)$.⁴ However, terminal diphenylhydrazido compounds of the 2nd and 3rd row Groups 6 (especially) and 7 metals have been extensively structurally characterized (ca. 40 such compounds are recorded in the Cambridge Structural Database).¹⁹

The $\text{Ti}(1)-\text{N}(1)$ bond length of $1.718(2) \text{ \AA}$ in **9** is equivalent, within experimental error, to the corresponding

**Figure 4.** Displacement ellipsoid plot (25% probability) of $\text{Ti}(\text{NNPh}_2)\text{Cl}_2\{\text{HC}(\text{Me}_2\text{pz})_3\}$ (**9**). Benzene molecules of crystallization and H atoms are omitted for clarity.

(23) Sandström, J. *Dynamic NMR Spectroscopy*; Academic Press: London, 1992.

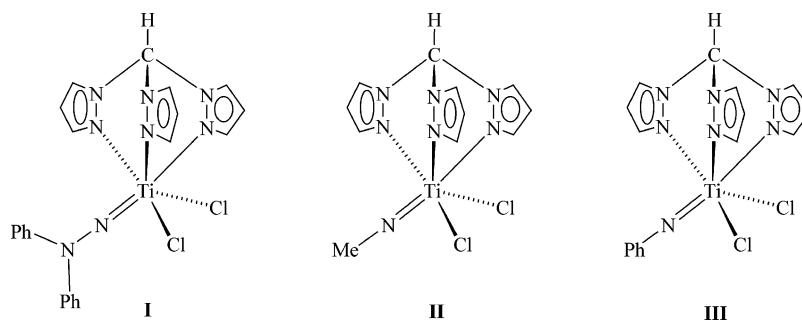


Figure 5. The model compounds $\text{Ti}(\text{NNPh}_2)\text{Cl}_2\{\text{HC}(\text{pz})_3\}$ (**I**) and $\text{Ti}(\text{NR})\text{Cl}_2\{\text{HC}(\text{pz})_3\}$ ($\text{R} = \text{Me}$ (**II**) or Ph (**III**)) used in the DFT calculations.⁹

Table 4. Selected Bond Lengths (Å) and Angles (deg) for $\text{Ti}(\text{NNPh}_2)\text{Cl}_2\{\text{HC}(\text{Me}_2\text{pz})_3\}$ (**9**)^a

Ti(1)–Cl(1)	2.4013(7)	Ti(1)–Cl(2)	2.3962(7)
Ti(1)–N(1)	1.718(2)	Ti(1)–N(3)	2.364(2)
Ti(1)–N(5)	2.242(2)	Ti(1)–N(7)	2.208(2)
N(1)–N(2)	1.369(3)		
Cl(1)–Ti(1)–Cl(2)	101.38(3)	Cl(1)–Ti(1)–N(1)	99.06(7)
Cl(2)–Ti(1)–N(1)	97.01(7)	Cl(1)–Ti(1)–N(3)	82.73(5)
Cl(2)–Ti(1)–N(3)	86.80(5)	N(1)–Ti(1)–N(3)	175.35(8)
Cl(1)–Ti(1)–N(5)	157.32(5)	Cl(2)–Ti(1)–N(5)	88.18(5)
N(1)–Ti(1)–N(5)	100.12(8)	N(3)–Ti(1)–N(5)	77.27(7)
Cl(1)–Ti(1)–N(7)	89.59(6)	Cl(2)–Ti(1)–N(7)	162.55(5)
Cl(2)–Ti(1)–N(7)	162.55(5)	N(1)–Ti(1)–N(7)	94.58(8)
N(3)–Ti(1)–N(7)	81.11(7)	N(5)–Ti(1)–N(7)	76.94(7)
Ti(1)–N(1)–N(2)	176.03(16)	Ti(1)–N(1)–N(2)	176.03(16)

^a Atoms carrying the suffix A are related their counterparts by the operator $[1 - x, y, 1/2 - z]$.

Table 5. Electron Occupancies of Selected NR Fragment Orbitals in $\text{Ti}(\text{NR})\text{Cl}_2\{\text{HC}(\text{pz})_3\}$ ($\text{NR} = \text{NNPh}_2$ (**I**), NMe (**II**), or NPh (**III**))^a

NR = NNPh ₂ (I)	
orbital (type)	occupancy
35A (π)	1.24
34A (π)	1.48
33A (π)	1.97
23A (σ)	1.80
NR = NMe (II)	
orbital (type)	occupancy
9A (π)	1.31
8A (π)	1.35
7A (σ)	1.59
NR = NPh (III)	
orbital (type)	occupancy
18A (π)	1.41
17A (π)	1.40
15A (π)	1.96
14A (σ)	1.74

^a The fragment orbital numbers correspond to those given in Figures 6 (**I**), 8 (**II**), and 9 (**III**), and the “type” given in parentheses refers to the generic symmetry of the interaction formed between the NR fragment orbital and the Ti center in $\text{TiCl}_2\{\text{HC}(\text{pz})_3\}$.

distance of 1.708(3) Å in $\text{Ti}(\text{NNMe}_2)(\text{dpma})(\text{tBu-bipy})$ and is also comparable to that typically found for titanium imido compounds (the usual $\text{Ti}=\text{NR}$ range is 1.69–1.74 Å¹⁹). Several imido analogues of **9** have been reported,^{22b,24} and in particular, we mention $\text{Ti}(\text{N}^t\text{Bu})\text{Cl}_2\{\text{HC}(\text{Me}_2\text{pz})_3\}$ (**10**) and $\text{Ti}(\text{NPh})\text{Cl}_2\{\text{HC}(\text{Me}_2\text{pz})_3\}$ (**11**) which have $\text{Ti}=\text{NR}$ distances of 1.703(2) and 1.719(2) Å.²⁴ The N(1)–N(2) distance of 1.369(3) Å in **9** is marginally shorter than the corresponding N–NMe₂ bond in $\text{Ti}(\text{NNMe}_2)(\text{dpma})(\text{tBu-bipy})$ (1.388(4) Å),

possibly indicating more N–N multiple-bond character in **9** (note that the NMe_2 nitrogen in $\text{Ti}(\text{NNMe}_2)(\text{dpma})(\text{tBu-bipy})$ is rather strongly pyramidalized (formally sp^3 hybridized), whereas N(2) in **9** is trigonal planar (sum of the angles subtended at N(2) is 359.9(6) °). The average N–NPh₂ distance in $\text{Cp}_2\text{Zr}(\text{NNPh}_2)(4\text{-NC}_5\text{H}_4\text{NMe}_2)$ is 1.363 Å (two independent molecules in the asymmetric unit with N–NPh₂ values of 1.350(3) and 1.376(3) Å), which is experimentally identical to that in **9**. However, for diphenylhydrazido compounds in general the average N–NPh₂ distance is 1.317 Å (range 1.275–1.376 Å).

Density Functional Theory Analysis of $\text{Ti}(\text{NNPh}_2)\text{Cl}_2\{\text{HC}(\text{pz})_3\}$ (I**) and a Comparison with Imido Compounds $\text{Ti}(\text{NMe})\text{Cl}_2\{\text{HC}(\text{pz})_3\}$ (**II**) and $\text{Ti}(\text{NPh})\text{Cl}_2\{\text{HC}(\text{pz})_3\}$ (**III**).** Computational studies of the bonding in transition metal hydrazido complexes are rare in comparison to those of the related imido systems.^{25,26} Previous computational studies²⁷ of metal–hydrazido(2–) bonding were based on extended Hückel calculations for hypothetical mono- and bis-hydrazido complexes, along with some ab initio calculations exploring the structure of $[\text{Li}(\text{NNH}_2)]^q$ ($q = +1, 0, \text{ or } -1$). In particular, these studies examined the bonding of the terminal hydrazido ligand in the model compound $[\text{MoH}_5(\text{NNH}_2)]^{3-}$ and compared the bonding between NNR end-on complexes with η^1 -bound NNR_2 species. No reports of DFT-based studies of terminal hydrazido complexes have appeared, and neither have direct comparisons been made between the electronic structures of hydrazido complexes and those of the corresponding imido complexes. Therefore, we describe in this contribution a DFT study of the bonding in $\text{Ti}(\text{NNPh}_2)\text{Cl}_2\{\text{HC}(\text{Me}_2\text{pz})_3\}$ (**9**), together with a comparison of that in the related imido complexes $\text{Ti}(\text{N}^t\text{Bu})\text{Cl}_2\{\text{HC}(\text{Me}_2\text{pz})_3\}$ (**10**) and Ti –

(24) (a) Sealey, A. J. PhD Thesis, University of Oxford, 2004. (b) Lawrence, S. C. PhD Thesis, University of Oxford, 2003.

(25) For a recent review of computational studies of transition metal–main group multiple bonding, see: Cundari, T. R. *Chem. Rev.* **2000**, *100*, 807.

(26) For examples of recent calculations of titanium terminal imido systems, see, in addition to refs 22a and b: (a) Boyd, C. L.; Clot, E.; Guiducci, A. E. Mountford, P. *Organometallics* **2005**, *24*, 2347. (b) Blake, A. J.; Cowley, A. R.; Dunn, S. C.; Green, J. C.; Hazari, N.; Jones, N. M.; Moody, A. G.; Mountford, P. *Chem.–Eur. J.* **2005**, *11*, 2111. (c) Kaltsoyannis, N.; Mountford, P. *J. Chem. Soc., Dalton Trans.* **1999**, 781. (d) Mountford, P.; Swallow, D. *J. Chem. Soc., Chem. Commun.* **1995**, 2357. (e) Zambrano, C. H.; Profflet, R. D.; Hill, J. E.; Fanwick, P. E.; Rothwell, I. P. *Polyhedron* **1993**, *12*, 689. (f) Cundari, T. R. *Organometallics* **1993**, *12*, 4971.

(27) (a) Kahlal, S.; Saillard, J.; Hamon, J.; Manzur, C.; Carrillo, D. *J. Chem. Soc., Dalton Trans.* **1998**, 1229. (b) Kahlal, S.; Saillard, J.; Hamon, J.; Manzur, C.; Carrillo, D. *New J. Chem.* **2001**, *25*, 231.

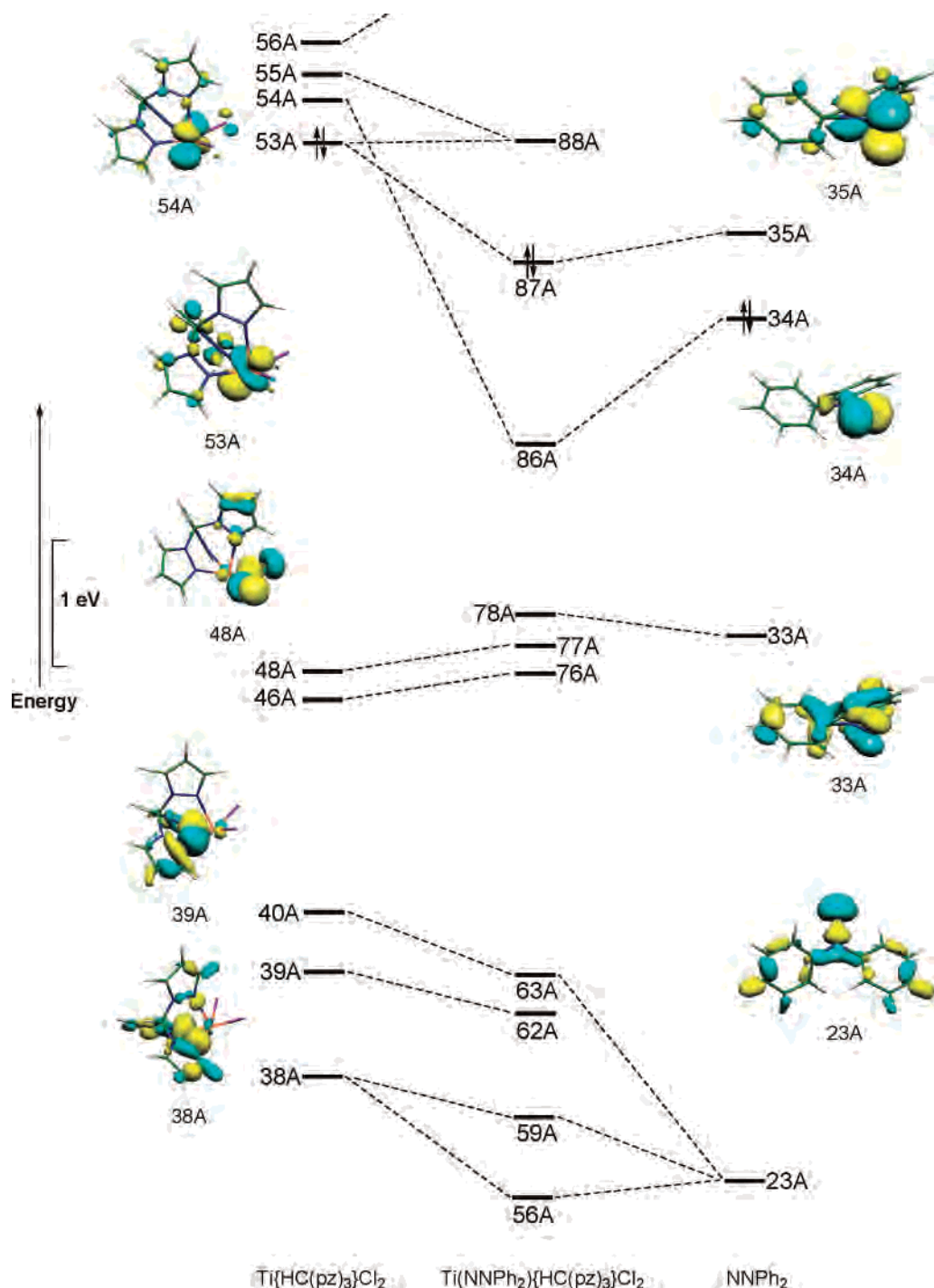


Figure 6. Fragment orbital-interaction diagram for $\text{Ti}(\text{NNPh}_2)\text{Cl}_2\{\text{HC}(\text{pz})_3\}$. The double arrows indicate the HOMO in the fragments and resultant complex.²⁸

$(\text{NPh})\text{Cl}_2\{\text{HC}(\text{Me}_2\text{pz})_3\}$ (**11**).²⁴ Finally, we also describe a DFT analysis of $\text{Ti}_2(\mu\text{-}\eta^2, \eta^1\text{-NNMe}_2)_2\text{Cl}_4(\text{HNMe}_2)_2$ (**2**).

The complex $\text{Ti}(\text{NNPh}_2)\text{Cl}_2\{\text{HC}(\text{pz})_3\}$ (**I**, Figure 5) was used as model for $\text{Ti}(\text{NNPh}_2)\{\text{HC}(\text{Me}_2\text{pz})_3\}\text{Cl}_2$ (**9**). $\text{Ti}(\text{NMe})\text{Cl}_2\{\text{HC}(\text{pz})_3\}$ (**II**) and $\text{Ti}(\text{NPh})\text{Cl}_2\{\text{HC}(\text{pz})_3\}$ (**III**) were used as models for the real compounds $\text{Ti}(\text{N}^t\text{Bu})\text{Cl}_2\{\text{HC}(\text{Me}_2\text{pz})_3\}$ (**10**) and $\text{Ti}(\text{NPh})\text{Cl}_2\{\text{HC}(\text{Me}_2\text{pz})_3\}$ (**11**), in a similar fashion. Except for hydrogen atoms, the experimental coordinates determined from the solid-state structure of **9** were used to describe the geometry of **I**. The positions of the hydrogen atoms were determined using a geometry optimization calculation in which all non-hydrogen atoms were fixed (no

symmetry restraints were imposed on this calculation). Compound **I** was divided into a neutral d^2 $\text{TiCl}_2\{\text{HC}(\text{pz})_3\}$ fragment and a neutral NNPh_2 fragment, and a fragment analysis performed. An orbital interaction diagram for **I** constructed from these fragments is shown in Figure 6.²⁸ Table 5 presents Mulliken populations (electron occupancies) of selected hydrazido fragment orbitals in complex **I**.

(28) Note that when NNPh_2 , NMe , or NPh bond to $\text{Ti}\{\text{HC}(\text{pz})_3\}\text{Cl}_2$ there is a net electron transfer from $\text{TiCl}_2\{\text{HC}(\text{pz})_3\}$ to NR which becomes partially negatively charged. In the fragment analysis, a neutral NR ligand is taken as one of the fragments (not a charged species) and as a result the energies of the NR orbitals increase upon bonding to the $\text{Ti}\{\text{HC}(\text{pz})_3\}\text{Cl}_2$ fragment.

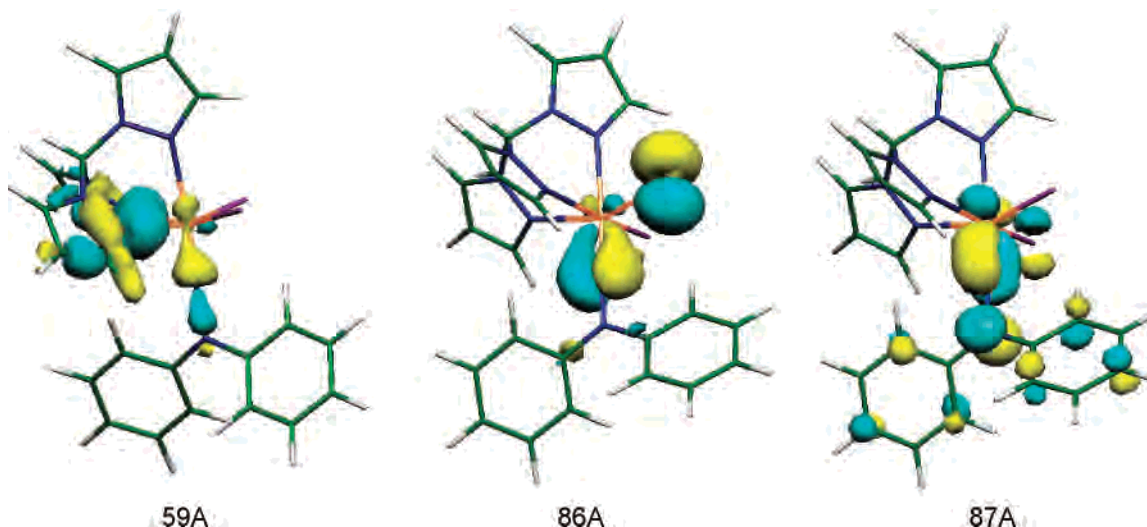


Figure 7. Representations of selected orbitals of $\text{Ti}(\text{NNPh}_2)\text{Cl}_2\{\text{HC}(\text{pz})_3\}$ (**I**).

The bonding in the neutral d^2 $\text{TiCl}_2\{\text{HC}(\text{pz})_3\}$ fragment is typical for a *pseudo* C_{4v} ML_5 fragment.²⁹ The tris-(pyrazolyl)methane ligand forms three low-lying σ bonds with the titanium center through one in-phase and two out-of-phase combinations of the lone pairs of the nitrogen atoms of the pyrazolyl rings (orbitals 38A, 39A, and 40A). The two chlorine atoms also form σ bonds with the titanium center (46A and 48A). This leaves four titanium-based orbitals which are available for bonding to another ligand (53A–56A). As a neutral d^2 Ti fragment is being considered, the lowest-energy orbital (53A) of these four orbitals is occupied.

As noted previously,²⁷ the NNPh_2 ligand has four frontier orbitals. Two of these (23A (σ type) and 34A (π type)) are associated with formal lone pairs on N_α (the N bound to Ti) and the other two represent the π_{NN} and π^*_{NN} orbitals (33A and 35A). Orbital 33A contains an antibonding interaction between the $2p_\pi$ AO of N_β and a π -bonding orbital of the phenyl rings. In the neutral fragment analysis, the π^*_{NN} orbital (35A) is unoccupied and represents the LUMO of the hydrazido fragment.

The principal interactions on formation of **I** from these fragments concern orbitals 38A, 39A, 40A, 53A, 54A, and 55A of $\text{TiCl}_2\{\text{HC}(\text{pz})_3\}$ and orbitals 23A, 34A, and 35A of NNPh_2 (Figure 6). Representations of the 59A, 86A, and 87A MOs of **I** are shown in Figure 7. Orbital 59A represents the principal σ interaction between Ti and the σ symmetry lone pair (orbital 23A) of the NNPh_2 . However, in the low symmetry of **I**, orbital 23A competes with the in-phase combination of the lone pairs of the $\text{HC}(\text{pz})_3$ ligand for the same titanium 3d orbitals. The resultant MO (59A) is therefore a combination of titanium-hydrazido σ bonding and titanium-tris(pyrazolyl)methane σ bonding. MOs 86A and 87A (Figure 7) represent the principal π interactions between NNPh_2 and Ti and are formed between two titanium-based orbitals (53A and 54A) of $\text{TiCl}_2\{\text{HC}(\text{pz})_3\}$ and the NNPh_2 fragment orbitals 34A ($2p_\pi$ lone pair on N_α) and 35A (π^*_{NN}

antibonding). Interestingly, however, the gap between the resulting π -bonding MOs, 87A and 86A, is rather large (1.38 eV). This is the result of the unfavorable antibonding interaction between N_α and N_β in 87A which is not present in 86A.

The NNPh_2 fragment orbital (33A, π_{NN} bonding), which is lower in energy than 34A and 35A, does not interact significantly with the metal and is Ti–N nonbonding in **I** (forming MO 78A). This is clearly seen from the 33A fragment orbital occupancy of 1.97 (Table 5) indicating negligible electron donation to titanium. Orbital 78A is thus responsible for the residual multiple-bond character of the N–N bond in **I**. However, the partial population of the NNPh_2 fragment N–N π^* -antibonding orbital 35A in **I** (occupancy 1.24, Table 5), reduces the N–N bond order and explains why the experimental N–N bond distance in the real complex **9** lies between typical N–N and N=N bond distances. The LUMO (orbital 88A) in the 16 valence electron compound **I** is based mainly on titanium and is nonbonding.

The $\text{Ti}=\text{NNPh}_2$ bonding description for **I** is in general agreement with the previous studies of metal-hydrazido bonding.²⁷ Overall, the hydrazido ligand formally donates 4 electrons to the metal (in a neutral electron-counting formalism) and forms one σ and two π bonds in an analogous fashion to that found for metal-imido bonding.^{25,26} However, it is clear that the presence of the NPh_2 moiety in **I** has a dramatic effect on the relative energies of the two $\text{Ti}=\text{N}_\alpha$ π -bonding orbitals (86A and 87A) because of unfavorable N–N π^* interactions in one of them (87A).

We turn now to a comparison of the bonding in **I** with that in the model alkyl- and aryl-imido compounds $\text{Ti}(\text{NMe})\text{Cl}_2\{\text{HC}(\text{pz})_3\}$ (**II**) and $\text{Ti}(\text{NPh})\text{Cl}_2\{\text{HC}(\text{pz})_3\}$ (**III**). Electronic-structure calculations for transition metal imido compounds in general²⁵ and for titanium specifically²⁶ have been described in detail previously. We note, especially, a recent DFT analysis (focusing in particular on trans influence trends) of the six-coordinate imido complexes $\text{Ti}(\text{NR})\text{Cl}_2(\text{NH}_3)_3$ ($\text{R} = \text{tBu, Ph, or } 4\text{-C}_6\text{H}_4\text{NO}_2$) as models of the real

(29) Albright, T. A.; Burdett, J. K.; Whangbo, M.-H. *Orbital Interactions in Chemistry*; Wiley-Interscience: New York, 1985.

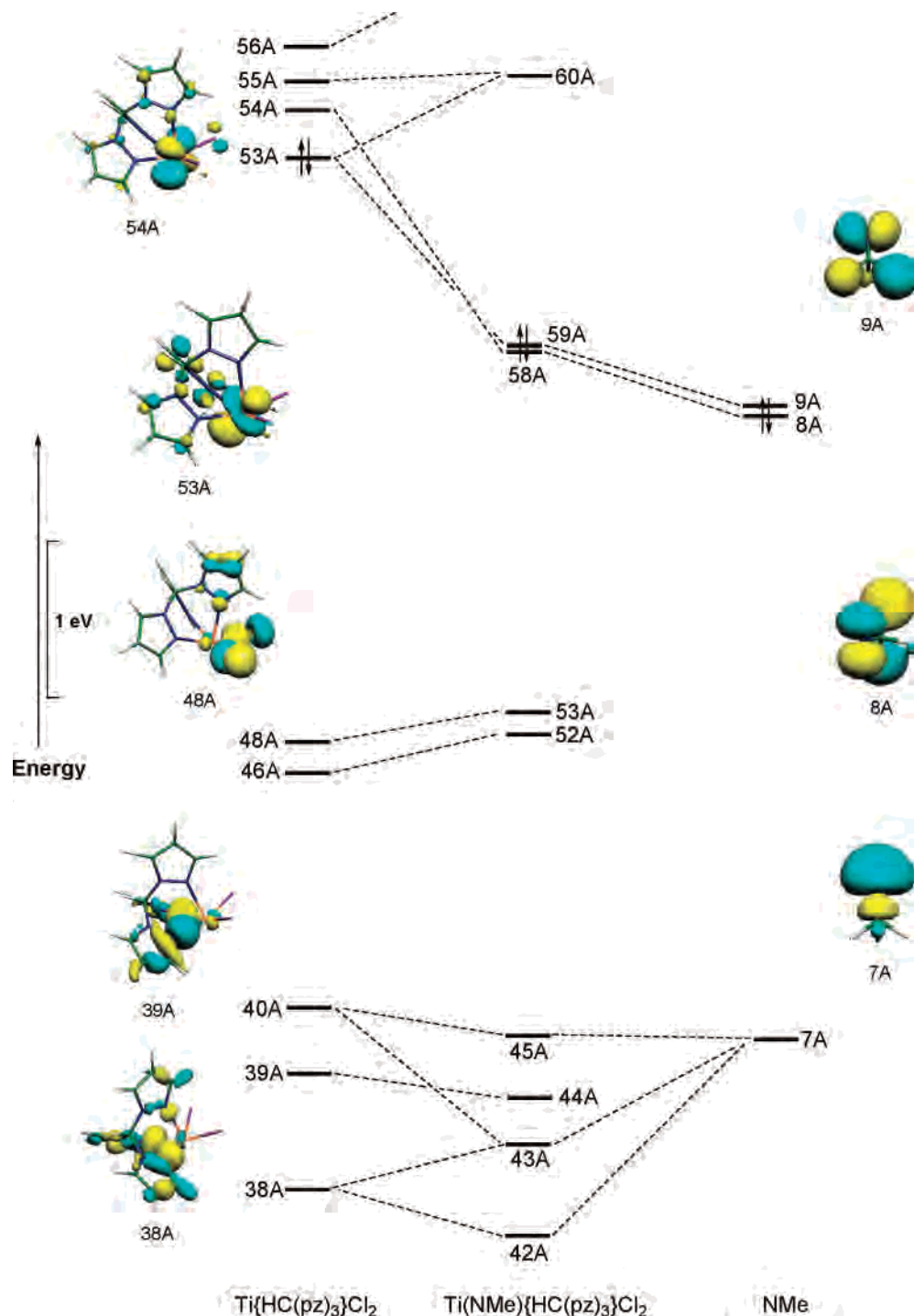


Figure 8. Fragment orbital-interaction diagram for $\text{Ti}(\text{NMe})\text{Cl}_2\{\text{HC}(\text{pz})_3\}$ (**II**). The double arrows indicate the HOMO in the fragments and resultant complex.²⁸

complexes $\text{Ti}(\text{NR})\text{Cl}_2(\text{py})_3$.^{26c} In our present contribution, therefore, we focus specifically on the similarities and differences in the $\text{Ti}=\text{NR}$ bonding and NR ligand donor ability in titanium-hydrazido (**I**) and -imido (**II** and **III**) systems.

To ensure that the analysis would be based only on electronic factors, we used the same supporting ligand–metal distances in all three systems. The coordinates obtained for the $\text{TiCl}_2\{\text{HC}(\text{pz})_3\}$ fragment in **I** were used to define the position of these atoms in calculations on **II** and **III**. The $\text{Ti}=\text{N}_{\text{imido}}$ bond distance was fixed at 1.716 Å (the experi-

mental value in **9** and that used in the calculations for **I**). The $\text{N}_{\text{imido}}-\text{C}$ bond lengths in **II** and **III** were, however, taken from the experimental structures of the real compounds $\text{Ti}(\text{NR})\text{Cl}_2\{\text{HC}(\text{Me}_2\text{pz})_3\}$ ($\text{R} = \text{tBu}$ ($\text{N}-\text{C}_{\text{Me}_3} = 1.448(3)$ Å) or Ph ($\text{N}-\text{C}_{\text{ipso}} = 1.378(3)$ Å)). The positions of all other atoms in compounds **II** and **III** were obtained through geometry optimization calculations (no symmetry restraints were imposed). Fragment analyses were performed on compounds **II** and **III** which were divided into neutral d^2 $\text{TiCl}_2\{\text{HC}(\text{pz})_3\}$ and NR ($\text{R} = \text{Me}$ or Ph) fragments. Fragment orbital-interaction diagrams for **II** and **III** are

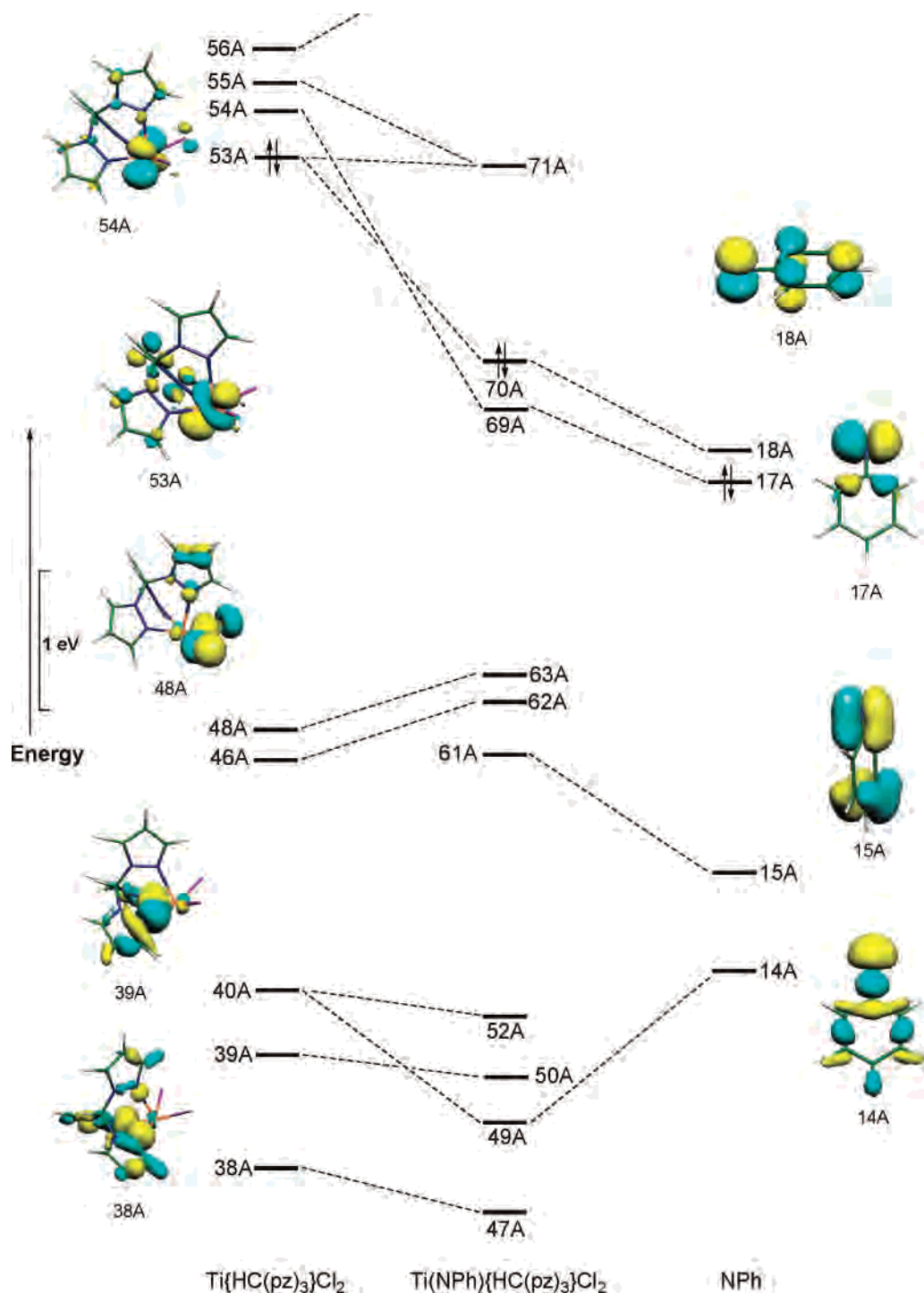


Figure 9. Fragment orbital-interaction diagram for $\text{Ti}(\text{NPh})\text{Cl}_2\{\text{HC}(\text{pz})_3\}$ (**III**). The double arrows indicate the HOMO in the fragments and resultant complex.²⁸

shown in Figures 8 and 9, respectively.²⁸ Table 5 lists selected NR fragment orbital occupancies (based on Mulliken analyses) for **II** and **III**.

The interactions between the $\text{TiCl}_2\{\text{HC}(\text{pz})_3\}$ and NR fragment orbitals in **II** (Figure 8) and **III** (Figure 9) are totally analogous to those in hydrazido compound **I** (i.e., metal fragment orbitals 38A–40A mix with the NR σ -donor fragment orbital while the $3d_{\pi}$ -acceptor orbitals 53A and 54A interact well with the $2p_{\pi}$ -donor orbitals). Therefore, in both **II** and **III**, the imido ligand forms the expected^{25,26} triple

bond (generic σ^2, π^4 configuration) with the metal center. The main difference between the orbital interaction diagrams for compounds **II** and **III** relates to the relative energies of the two $\text{Ti}=\text{NR}$ π -bonding orbitals. These are essentially isoenergetic in **II** (orbitals 58A and 59A, separation 0.06 eV) but are separated by 0.32 eV in **III** (orbitals 69A and 70A). This difference in energy in **III** is the result of an unfavorable π^* -antibonding interaction in 70A between the $2p_{\pi}$ orbital of the nitrogen and one of the π -bonding orbitals of the phenyl ring. Orbital 69A lies in the plane of the phenyl

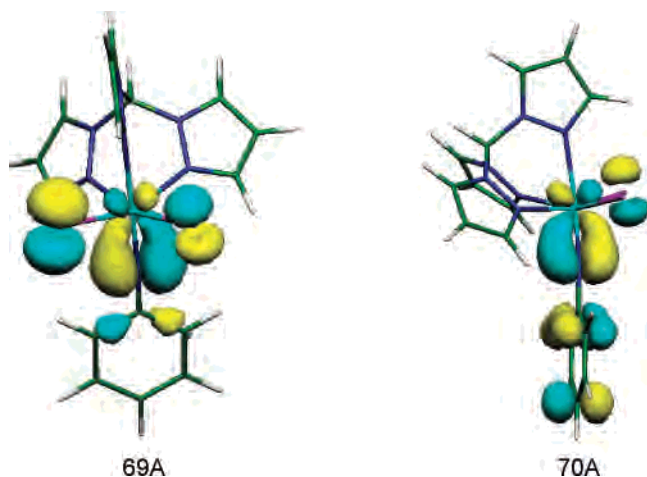


Figure 10. Representations of the Ti–N π -bonding orbitals 69A and 70A in $\text{Ti}(\text{NPh})\text{Cl}_2\{\text{HC}(\text{pz})_3\}$ (**III**). Note the N–Ph antibonding interaction in 70A.

ring and experiences no such destabilization. Representations of orbitals 69A and 70A of compound **III** are shown in Figure 10

We have recently noted the same destabilizing feature of titanium–arylimido bonding in $\text{Ti}(\eta^8\text{-C}_8\text{H}_8)(N\text{-}2,6\text{-C}_6\text{H}_3\text{-i-Pr}_2)$.^{26b} As expected, the fragment $2p_\pi$ -donor orbitals of NPh (17A and 18A in Figure 9) are also separated in energy because of this unfavorable N–phenyl antibonding interaction. The NPh fragment orbital 15A represents the corresponding N–phenyl π -bonding combination. In complex **III**, this latter orbital (which lies low in energy compared to 17A and 18A) has an occupancy of 1.96 electrons (Table 5) showing that it contributes little to the Ti–NPh bonding. The destabilizing effect of the N–phenyl π^* interaction present in the 70A molecular orbital (HOMO) of **III** is analogous to the $N_\alpha\text{-}N_\beta$ π^* -antibonding contribution to 87A molecular orbital (HOMO) in the hydrazido complex **I**. In **I**, the destabilizing effect is much more significant ($\Delta(\text{HOMO}) - (\text{HOMO}-1) = 1.38$ eV in **I** vs 0.32 eV in **III**). Therefore of the three $\text{Ti}(\text{NR})\text{Cl}_2\{\text{HC}(\text{pz})_3\}$ compounds studied, only the alkyl imide **II** has a Ti–NR bond that is free of π^* -antibonding contributions from the R substituent (R = NPh₂ or Ph).

To evaluate the relative donor abilities of the hydrazido and imido ligands in the three compounds, **I–III**, we considered the Mulliken populations (occupancies) of the σ - and π -donor orbitals of the NR fragments, as well as the net (atom–atom) Ti–N overlap populations and NR fragment Hirshfeld charges.³⁰

The NR fragment σ - and π -donor orbital occupancies in **I–III** are summarized in Table 5. For these particular fragment orbitals, an occupancy of 2 electrons in the resultant complex indicates that the orbital is not involved in electron donation to titanium. Correspondingly, an electron occupancy of less than 2 represents donation of electron density to titanium relative to the formally dianionic NR^{2-} hydrazide or imide and dicationic $[\text{TiCl}_2\{\text{HC}(\text{pz})_3\}]^{2+}$. As mentioned

Table 6. Net Extent of NR Ligand σ and π Donation (electrons), Ti–N Mulliken Overlap Populations (OPs) and Hirshfeld³⁰ NR Fragment Charges in $\text{Ti}(\text{NR})\text{Cl}_2\{\text{HC}(\text{pz})_3\}$ (NR = NNPh₂ (**I**), NMe (**II**), or NPh (**III**))

	σ donation	π donation	total	OP	charge NR
I	0.20	1.28	1.58	0.34	−0.49
II	0.41	1.34	1.75	0.39	−0.48
III	0.26	1.19	1.45	0.27	−0.55

Table 7. Electron Occupancies of Selected NNMe₂ Fragment Orbitals in $\text{Ti}_2(\mu\text{-}\eta^2\text{-}\eta^1\text{-NNMe}_2)_2\text{Cl}_4(\text{HNMe}_2)_2$ (**2**) for Both NNMe₂ Fragments

orbital	type	occupancy fragment 1	occupancy fragment 2
13A	N–N antibonding (π)	1.22	1.23
12A	N_α lone pair (π)	1.46	1.46
11A	N–N bonding (π)	1.83	1.84
10A	N_α lone pair (σ)	1.80	1.80

above, the occupancy of 1.97 electrons for orbital 33A ($N_\alpha\text{-}N_\beta$ π bonding) of **I** and 1.96 electrons for orbital 15A (N–phenyl π bonding) of **III** show that the contribution of these fragment orbitals to Ti–NR π bonding is negligible. An analysis of the σ -orbital occupancies shows that the σ -donor ability of the three fragments decreases in the order NMe > NPh > NNPh₂. For the corresponding π -donor abilities, one should consider all of the π fragment orbitals and Table 6 summarizes these data in terms of total electrons formally donated (i.e., $\sum(2 - \text{orbital occupancy})$). In terms of π -donor ability, the order is NMe > NNPh₂ > NPh, and for overall σ and π donation combined, NMe is best donor, followed by NNPh₂, with NPh being the poorest electron donor for the systems under consideration. The donor ability inferred from the orbital occupancy analysis is supported by the Ti–N atom–atom overlap populations listed in Table 6 (Ti–N(R) for R = Me > NPh₂ > Ph) and the NR fragment charges (least negative for NR = NMe followed by NNPh₂ and then NPh). This order of NR-group donor ability is consistent with the bond lengths found in the real complexes $\text{Ti}(\text{NR})\text{-Cl}_2\{\text{HC}(\text{Me}_2\text{pz})_3\}$ (R = ^tBu < Ph \approx NNPh₂), and with the general observation^{26c} that, for homologous pairs of compounds, M = N^tBu bond lengths are typically significantly shorter than the corresponding M = NPh bond lengths.

DFT Analysis of $\text{Ti}_2(\mu\text{-}\eta^2\text{-}\eta^1\text{-NNMe}_2)_2\text{Cl}_4(\text{HNMe}_2)_2$ (2**).** The electronic structure of the crystallographically characterized $\text{Ti}_2(\mu\text{-}\eta^2\text{-}\eta^1\text{-NNMe}_2)_2\text{Cl}_4(\text{HNMe}_2)_2$ (**2**) was compared with that of compound **9**. Except for hydrogen atoms, the experimental coordinates determined from the solid-state structure of **2** were used to describe its geometry. The positions of the hydrogen atoms were determined using a geometry optimization calculation in which all non-hydrogen atoms were fixed (no symmetry restraints were imposed). A fragment analysis was performed where **2** was divided into two equivalent NNMe₂ fragments (each fragment representing one of the bridging hydrazides) and into a TiCl_2 and a $\text{TiCl}_2(\text{HNMe}_2)_2$ fragment. Table 7 lists selected NNMe₂ fragment orbital occupancies (based on Mulliken analyses) for **2**.

In a fashion analogous to that of **I**, both the hydrazido fragments of **2** have four orbitals each that are suitable for bonding to the two titanium centers. Overall, this results in eight hydrazido orbitals that are combinations of the two

(30) (a) Hirshfeld, F. L. *Theor. Chim. Acta* **1977**, *44*, 129. (b) Wiberg, K. B.; Rablen, P. R. *J. Comput. Chem.* **1993**, *14*, 1504.

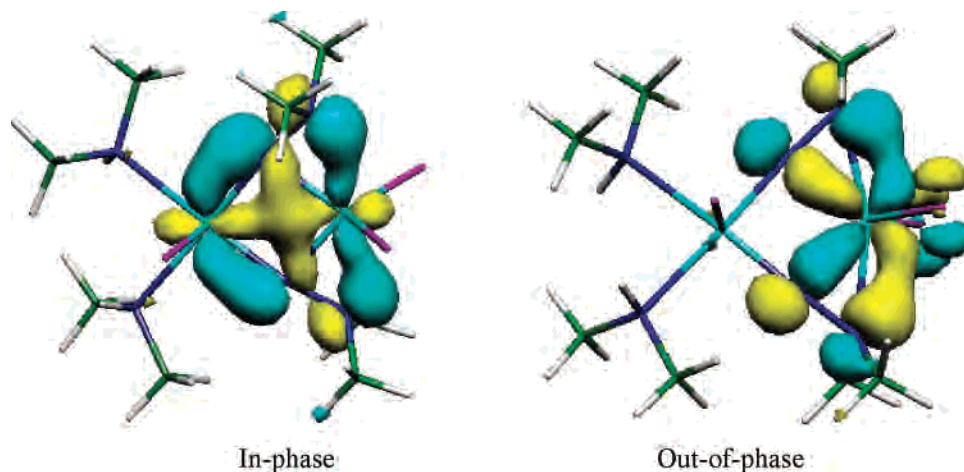


Figure 11. In-phase and out-of-phase combinations of the two π^*_{NN} orbitals of $\text{Ti}_2(\mu\text{-}\eta^2, \eta^1\text{-NNMe}_2)_2\text{Cl}_4(\text{HNMe}_2)_2$ (**2**).

hydrazido fragments which can be used for bonding to the metal centers. These eight orbitals consist of an in-phase and out-of-phase combination for each of the two lone pairs on the two N_α atoms (two of these orbitals are σ and two are π in symmetry) and an in-phase and out-of-phase combination for the two π_{NN} -bonding and two π^*_{NN} -antibonding orbitals.

The σ lone pairs on the two N_α atoms (both the in-phase and out-of-phase combinations) only interact with one titanium center (that with the two-coordinated amines). Both of these orbitals mix with the amine ligands and the titanium 3d orbitals to form metal–ligand σ bonds in a fashion similar to **1**. In contrast, the in-phase and out-of-phase combinations of the π lone pairs on the two N_α atoms form π bonds with both metal centers. The π_{NN} hydrazido-bonding orbitals mix with the π lone pairs on the two N_α atoms and the two π^*_{NN} -bonding orbitals to interact with the metal centers. This is clearly indicated in Table 7 which shows that the occupancies of the π_{NN} hydrazido-bonding orbitals in **2** are 1.83 and 1.84, and this is the major difference between the bonding in **2** and the bonding in **1** (occupancy π_{NN} in **1** is 1.96). The occupancies of the other hydrazido-bonding orbitals in **2** are very similar to their corresponding orbitals in **1**. Interestingly, the in-phase and out-of-phase combinations of the two π^*_{NN} -bonding orbitals bond differently to the titanium centers. The in-phase combination bonds to both of the titanium centers, whereas the out-of-phase combination only bonds to one of the titanium centers. Representations of these orbitals are shown in Figure 11.

Overall, the electronic structure of **2** clearly shows the asymmetric nature of the two bridging hydrazido ligands. One of the titanium centers only bonds to N_α (the center with the coordinated amines), while the other center bonds to both N_α and N_β . It is possible to describe the interaction between the hydrazido fragment and the titanium center which binds both N_α and N_β in two different ways as shown in Figure 12. In mode a, the hydrazido ligands bond to the metal center through a π interaction, whereas in mode b, a three-membered metallocycle is formed. In complex **2**, the bonding is probably better described by mode b than by a. There are clear σ -interactions between both N_α and N_β and the Ti center as shown in Figure 11, suggesting a metallocyclic structure. Also, the partial population of the π^*_{NN} , as

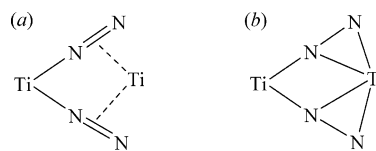


Figure 12. Potential bonding modes of the bridging hydrazido ligand. shown in Table 7, indicates a reduction in the N–N bond order and provides further support for bonding mode b.

Conclusions

We have established a new class of titanium hydrazido(2-) complexes through synthetic, structural, and DFT studies. The titanium terminal hydrazido compound $\text{Ti}(\text{NNPh})\text{Cl}_2(\text{HNMe}_2)_2$ (**1**) has been developed and shown to undergo facile metathesis reactions with a number of *fac*- N_3 donor ligands to produce further new hydrazido complexes. One of these, $\text{Ti}(\text{NNPh}_2)\text{Cl}_2\{\text{HC}(\text{Me}_2\text{pz})_3\}$ (**9**), represents only the second crystallographically characterized terminal hydrazido complex of titanium. A second potential synthon $[\text{Ti}(\text{NNPh}_2)\text{Cl}_2(\text{py})_2]_n$ (**4**) has also been developed, and it also undergoes methathesis reactions. Reduction of the steric bulk on the hydrazido ligand leads to unsymmetrical dimeric species with bridging $\mu\text{-}\eta^2, \eta^1$ -bound hydrazido ligands, and three of these have been crystallographically characterized. These dimeric species do not undergo metathesis reactions with neutral *fac*- N_3 donor ligands.

The DFT analysis of the electronic structures of the terminal hydrazido and imido complexes $\text{Ti}(\text{NR})\text{Cl}_2\{\text{HC}(\text{pz})_3\}$ ($\text{R} = \text{NPh}_2, \text{Me}, \text{or Ph}$) showed that the NNPh_2 ligand binds to the metal center in a manner analogous to that of the terminal imido ligands but with one of the $\text{Ti}=\text{N}$ π components significantly destabilized by the formal lone pair of the $\beta\text{-N}$ atom. The NR σ -donor ability was found to be $\text{NMe} > \text{NPh} > \text{NNPh}_2$, whereas the overall ($\sigma + \pi$) donor ability is $\text{NMe} > \text{NNPh}_2 > \text{NPh}$ as determined from fragment orbital population, overlap population, and fragment charge analysis. The principal difference in orbital occupancy when the hydrazido ligand is bonding in a bridging mode is donation of the $\text{N}=\text{N}$ π -bonding electrons to one of the Ti centers. The TiN_2 interaction is best represented as a metallocycle because back donation into the $\text{N}=\text{N}$ π^* orbital is extensive.

The chemistry of the Ti=NR (imido) bond has been developed in some detail over the past decade in particular,⁶ while that of the Ti=NNR₂ (hydrazido) bond is virtually unexplored.^{2a} Much of the chemistry of the Ti=NR bond involves [2 + 2] cycloaddition reactions with electrophilic substrates. Our DFT analysis suggests that the Ti=NNR₂ bond should, for otherwise analogous systems, be more reactive in this regard because of the destabilizing effect of the N_α-N_β π*-antibonding contribution to the HOMO. Our future efforts in this area will be aimed at developing the reaction chemistry of the Ti=NNR₂ multiple bond.

Experimental Section

General Methods and Instrumentation. All manipulations were carried out using standard Schlenk line or drybox techniques under an atmosphere of argon or dinitrogen. Solvents were predried over activated 4 Å molecular sieves and were refluxed over appropriate drying agents under a dinitrogen atmosphere and collected by distillation. Deuterated solvents were dried over appropriate drying agents, distilled under reduced pressure, and stored under dinitrogen in Teflon valve ampules. NMR samples were prepared under dinitrogen in 5 mm Wilmad 507-PP tubes fitted with J. Young Teflon valves. ¹H and ¹³C NMR spectra were recorded on a Varian Mercury 500 spectrometer with a probe temperature of 298 K. ¹H and ¹³C assignments were confirmed when necessary with the use of nOe and two-dimensional ¹H-¹H and ¹³C-¹H NMR experiments. All spectra were referenced internally to residual protio-solvent (¹H) or solvent (¹³C) resonances and are reported relative to tetramethylsilane (δ = 0 ppm). Chemical shifts are quoted in δ (ppm) and coupling constants in hertz. Infrared spectra were prepared as Nujol mulls between NaCl plates and were recorded on Perkin-Elmer 1600 and 1700 series spectrometers. Infrared data are quoted in wave-numbers (cm⁻¹). Mass spectra were recorded by the mass spectrometry service of the University of Oxford's Department of Chemistry. Combustion analyses were recorded by the elemental analysis service at the London Metropolitan University.

Starting Materials. The compounds Ti(NMe₂)₂Cl₂,¹⁰ Me₃[9]-aneN₃,³¹ Me₃[6]aneN₃,³² HC(Me₂pz)₃,³³ HC(ⁿBupz)₃,³⁴ and Ti(N^t-Bu)Cl₂(py)₃²⁰ were prepared by literature methods. Diphenylhydrazine was purified as described previously.^{2g} Dimethylhydrazine, *N*-aminopiperidine, and pyridine were dried over freshly ground CaH₂ and distilled before use. Other reagents were obtained from Sigma-Aldrich and used as received.

Ti(NNPh₂)Cl₂(HNMe₂)₂ (1). A solution of H₂NNPh₂ (1.55 g, 8.43 mmol) in benzene (40 mL) was added to a stirred solution of TiCl₂(NMe₂)₂ (1.74 g, 8.43 mmol) in benzene (40 mL) over 30 min. The reaction mixture immediately turned a dark orange-brown color and was left to stir for a further period during which time there was no additional color change. The solution was filtered, and the volatiles were removed under reduced pressure to give **1** as a brown-green powder. Yield: 3.00 g (91%). ¹H NMR (C₆D₆, 500.0 MHz): δ 7.68 (4H, m, *ortho-H*), 7.22 (4H, m, *meta-H*), 6.86 (2H, m, *para-H*), 2.79 (2H, sep, ³J = 6.3 Hz, *NHMe*₂), 2.19 (12H, d, ³J = 6.3 Hz, *NHMe*₂). ¹³C-{¹H} NMR (C₆D₆, 125.8 MHz): δ

145.3 (*ipso-C*), 129.6 (*meta-C*), 123.9 (*para-C*), 118.2 (*ortho-C*), 41.4 (*NHMe*₂). IR (NaCl plates, Nujol mull, cm⁻¹): ν 3254 (br, w), 1588 (w), 1492 (w), 1092 (br, m), 1018 (br, m), 800 (w). EI-MS: *m/z* 168 [NPh₂]⁺ (73%), 105 [NNPh]⁺ (2%). Anal. Found (calcd) for C₁₆H₂₄Cl₂N₄Ti: C, 49.0 (49.1); H, 6.1 (6.2); N, 14.3 (14.3).

Ti₂(μ-η²,η¹-NNMe₂)₂Cl₄(HNMe₂)₂ (2). H₂NNMe₂ (0.25 g, 4.11 mmol) was added to a stirred brown solution of TiCl₂(NMe₂)₂ (0.85 g, 4.11 mmol) in benzene (25 mL). The resultant deep red mixture was left to stir for 2 h, after which a precipitate had formed. The supernatant was decanted and the residues dried in vacuo give **2** as a red powder. Yield: 0.60 g (66%). ¹H NMR (CD₂Cl₂, 500.0 MHz): δ 3.68 (2H, m, br, *HNMe*₂), 3.45 (12H, s, *NNMe*₂), 2.47 (12H, d, ³J = 5.9 Hz *HNMe*₂). ¹³C-{¹H} NMR (CD₂-Cl₂, 125.8 MHz): δ 52.7 (*NNMe*₂), 42.6 (*HNMe*₂). IR (NaCl plates, Nujol mull, cm⁻¹): ν 3268 (w), 1632 (br, w), 1306 (w), 1260 (sh, m), 1096 (br, m), 1019 (m), 987 (w), 896 (w), 803 (m), 722 (w). EI-MS: *m/z* 354 [Ti₂(NNMe₂)₂Cl₄]⁺ (17%), 216 [Ti₂(NNMe₂)₂]⁺ (5%), 58 [NNMe₂]⁺ (100%). Anal. Found (calcd) for C₈H₂₆Cl₄N₆-Ti₂: C, 23.5 (23.5); H, 6.1 (6.0); N, 18.4 (18.4).

Ti₂{μ-η²,η¹-NN(CH₂)₅}₂Cl₄(HNMe₂)₃ (3). A solution of *N*-aminopiperidine (0.24 g, 2.40 mmol) in benzene (15 mL) was added to a stirred brown solution of TiCl₂(NMe₂)₂ (0.49 g, 2.39 mmol) in benzene (25 mL) over 10 min. The resultant crimson mixture was left to stir for 16 h. The supernatant was decanted, and the crimson solid washed with benzene (20 mL). Drying in vacuo produced **3** as an orange powder. Yield: 0.42 g (62%). ¹H and ¹³C NMR data could not be obtained as **3** was insoluble in nonreactive NMR solvents. IR (NaCl plates, Nujol mull, cm⁻¹): ν 3241 (w), 1613 (br, w), 1307 (w), 1260 (m), 1093 (br, m), 1022 (br, m), 898 (w), 851 (w), 801 (m), 722 (w), 683 (w). EI-MS: *m/z* 434 [Ti₂-{NN(CH₂)₅}₂Cl₄]⁺ (64%), 84 [N(CH₂)₅]⁺ (100%). Anal. Found (calcd) for C₁₆H₄₁Cl₄N₇Ti₂: C, 33.9 (33.8); H, 7.2 (7.3); N, 17.2 (17.2).

[Ti(NNPh₂)Cl₂(py)₂]_n (4). A solution of Ti(NNPh₂)Cl₂(HNMe₂)₂ (**1**) (1.01 g, 2.58 mmol) in pyridine (40 mL) was heated for 16 h at 70 °C. The dark yellow-brown solution was filtered, and the volatiles were removed under reduced pressure to yield crude **4** as a yellow-green solid. This was washed with benzene (20 mL), and the volatiles were removed under reduced pressure to give **4** as a yellow-green powder. Yield: 1.01 g (87%). ¹H NMR (CD₂Cl₂, 500.0 MHz): δ 9.01 (4H, app d, *py ortho-H*), 7.82 (2H, m, *py para-H*), 7.43 (4H, m, *ortho-H*), 7.37 (4H, m, *py meta-H*), 7.26 (4H, m, *meta-H*), 6.99 (2H, m, *para-H*). ¹³C-{¹H} NMR (CD₂Cl₂, 125.8 MHz): δ 152.0 (*py ortho-C*), 149.7 (*py para-C*), 144.4 (*ipso-C*), 129.1 (*meta-C*), 124.6 (*py meta-C*), 123.5 (*para-C*), 118.8 (*ortho-C*). IR (NaCl plates, Nujol mull, cm⁻¹): ν 1601 (br, w), 1260 (m), 1092 (br, w), 1021 (br, m), 803 (m), 722 (m). EI-MS: *m/z* 168 [NPh₂]⁺ (100%), 153 [TiNNPh]⁺ (28%). Anal. Found (calcd) for C₂₂H₂₀Cl₂N₄Ti: C, 57.5 (57.5); H, 4.3 (4.4); N, 12.3 (12.2).

Ti₂(μ-η²,η¹-NNMe₂)₂Cl₄(py)₂ (5). H₂NNMe₂ (70.3 mg, 1.17 mmol) was added to a stirred orange solution of Ti(N^tBu)Cl₂(py)₃ (0.50 g, 1.17 mmol) in benzene (40 mL). The dark reaction mixture was stirred for 90 min, after which a precipitate had formed. The solution was concentrated to approximately 20 mL and left to stir for a further 30 min. Filtration yielded **5** as an orange powder, which was dried in vacuo. Yield: 0.14 g (45%). ¹H NMR (CD₂Cl₂, 500.0 MHz): δ 8.95 (4H, m, br, *ortho-H*), 7.87 (2H, m, *para-H*), 7.40 (4H, m, *meta-H*), 3.48 (12H, s, *NNMe*₂). ¹³C-{¹H} NMR (CD₂Cl₂, 125.8 MHz): δ 154.4 (*ortho-C*), 139.3 (*para-C*), 124.7 (*meta-C*), 51.4 (*NNMe*₂). IR (NaCl plates, Nujol mull, cm⁻¹): ν 1624 (br, w), 1260 (sh, m), 1091 (br, m), 1019 (br, m), 800 (m), 722 (w).

(31) Madison, S. A.; Batal, D. J.; Unilever PLC, U.K.; Unilever N. V. U.S. Patent 5,284,944, 1994.

(32) Hoerr, C. W.; Rapkin, E.; Brake, A. E.; Warner, K. N.; Harwood, H. J. *J. Am. Chem. Soc.* **1956**, *78*, 4667.

(33) Reger, D. L.; Grattan, T. C.; Brown, K. J.; Little, C. A.; Lamba, J. J. S.; Rheingold, A. L.; Sommer, R. D. *J. Organomet. Chem.* **2000**, *607*, 120.

(34) Selby, J. D.; Mountford, P. Manuscript in preparation.

EI-MS: m/z 354 $[\text{Ti}_2(\text{NNMe}_2)_2\text{Cl}_4]^+$ (17%), 216 $[\text{Ti}_2(\text{NNMe}_2)_2]^+$ (5%), 58 $[\text{NNMe}_2]^+$ (100%). Anal. Found (calcd) for $\text{C}_{14}\text{H}_{22}\text{Cl}_4\text{N}_6$ - Ti_2 : C, 32.7 (32.9); H, 4.4 (4.3); N, 16.4 (16.4).

Ti₂{ μ - η^2 , η^1 -NN(CH₂)₅}₂Cl₄(py)₂ (6). A solution of *N*-aminopiperidine (0.12 g, 1.15 mmol) in benzene (10 mL) was added to a stirred orange solution of $\text{Ti}(\text{N}^i\text{Bu})\text{Cl}_2(\text{py})_3$ (0.49 g, 1.15 mmol) in benzene (50 mL) over 10 min. The resultant bright red solution was left to stir for 16 h, after which an orange solid had formed. The supernatant was decanted, and the solid was washed with benzene (20 mL) and dried in vacuo give **6** as an orange powder. Yield: 0.24 g (68%). ¹H and ¹³C NMR data could not be obtained as **6** was insoluble in nonreactive NMR solvents. IR (NaCl plates, Nujol mull, cm⁻¹): ν 1652 (br, w), 1601 (w), 1260 (m), 1091 (br, m), 1026 (br, m), 802 (br, w), 722 (w), 697 (w). EI-MS: m/z 434 $[\text{Ti}_2\{\text{NN}(\text{CH}_2)_5\}_2\text{Cl}_4]^+$ (100%), 84 $[\text{N}(\text{CH}_2)_5]^+$ (90%). Anal. Found (calcd) for $\text{C}_{20}\text{H}_{30}\text{Cl}_4\text{N}_6\text{Ti}_2$: C, 40.6 (40.6); H, 5.0 (5.1); N, 14.4 (14.2).

Ti(NNPh₂)Cl₂(Me₃[9]aneN₃) (7). A solution of Me₃[9]aneN₃ (0.25 g, 1.46 mmol) in benzene (5 mL) was added to a stirred solution of $\text{Ti}(\text{NNPh}_2)\text{Cl}_2(\text{HNMe}_2)_2$ (**1**) (0.57 g, 1.46 mmol) in benzene (20 mL) over 15 min. On addition of the ligand, the reaction mixture changed from an orange-brown solution to a yellow suspension. The mixture was stirred for a further 90 min and then filtered. Volatiles were removed under reduced pressure, giving **7** as a light yellow-green powder. Yield: 0.56 g (81%). ¹H NMR (CD₂Cl₂, 500.0 MHz): δ 7.41 (4H, m, *ortho-H*), 7.32 (4H, m, *meta-H*), 7.02 (2H, m, *para-H*), 3.15 (2H, m, NMe_{cis}CH₂CH₂NMe_{trans} down), 3.05 (2H, m, NMe_{cis}CH₂CH₂NMe_{cis} down), 3.01 (2H, m, NMe_{cis}CH₂CH₂NMe_{trans} down), 2.84 (6H, s, NMe_{cis}), 2.75 (2H, m, NMe_{cis}CH₂CH₂NMe_{cis} up), 2.64 (2H, m, NMe_{cis}CH₂CH₂NMe_{trans} up), 2.56 (3H, s, NMe_{trans}), 2.48 (2H, m, NMe_{cis}CH₂CH₂NMe_{trans} up). ¹³C-¹H NMR (CD₂Cl₂, 125.8 MHz): δ 146.7 (*ipso-C*), 129.7 (*ortho-C*), 124.1 (*para-C*), 121.2 (*meta-C*), 57.4 (NMe_{cis}CH₂CH₂-NMe_{trans}), 57.1 (NMe_{cis}CH₂CH₂NMe_{cis}), 55.8 (NMe_{cis}CH₂CH₂-NMe_{trans}), 53.7 (NMe_{trans}, partially obscured by solvent), 49.8 (NMe_{cis}). IR (NaCl plates, Nujol mull, cm⁻¹): ν 1585 (w), 1260 (m), 1092 (br, w), 1020 (br, w), 802 (m), 722 (w). EI-MS: m/z 471 $[\text{M}]^+$ (17%), 289 $[\text{M}-\text{NNPh}_2]^+$ (14%), 168 $[\text{NPh}_2]^+$ (39%). HR EI-MS found (calcd) for $\text{C}_{21}\text{H}_{31}\text{Cl}_2\text{N}_5\text{Ti}$: m/z 471.1423 (471.1436). Anal. Found (calcd) for $\text{C}_{21}\text{H}_{31}\text{Cl}_2\text{N}_5\text{Ti}$: C, 53.3 (53.4); H, 6.5 (6.6); N, 14.7 (14.8).

Ti(NNPh₂)Cl₂(Me₃[6]aneN₃) (8). A solution of Me₃[6]aneN₃ (99.0 mg, 0.77 mmol) in benzene (5 mL) was added to a stirred solution of $\text{Ti}(\text{NNPh}_2)\text{Cl}_2(\text{HNMe}_2)_2$ (**1**) (0.30 g, 0.77 mmol) in benzene (20 mL) over 5 min to form a green precipitate. After 16 h, the supernatant was decanted to leave **8** as a green powder which was dried in vacuo. Yield: 0.25 g (76%). ¹H NMR (CD₂Cl₂, 500.0 MHz): δ 7.47 (4H, m, *ortho-H*), 7.32 (4H, m, *meta-H*), 6.99 (2H, m, *para-H*), 4.24 (2H, d, ²J = 8.0 Hz, NMe_{cis}CH₂NMe_{trans} up), 4.03 (1H, d, ²J = 7.7 Hz, NMe_{cis}CH₂NMe_{cis} up), 3.40 (1H, d, ²J = 7.7 Hz, NMe_{cis}CH₂NMe_{cis} down), 3.25 (2H, d, ²J = 8.0 Hz, NMe_{cis}CH₂NMe_{trans} down), 2.51 (6H, s, NMe_{cis}), 2.13 (3H, s, NMe_{trans}). ¹³C-¹H NMR (CD₂Cl₂, 125.8 MHz): δ 145.3 (*ipso-C*), 129.6 (*ortho-C*), 123.6 (*para-C*), 119.2 (*meta-C*), 78.9 (NMe_{cis}CH₂NMe_{trans}), 76.8 (NMe_{cis}CH₂NMe_{cis}), 41.9 (NMe_{trans}), 37.5 (NMe_{cis}). IR (NaCl plates, Nujol mull, cm⁻¹): ν 1594 (w), 1260 (m), 932 (sw), 802 (m). EI-MS: m/z 429 $[\text{M}]^+$ (2%), 168 $[\text{NPh}_2]^+$ (100%), 129 $[\text{Me}_3[6]\text{aneN}_3]^+$ (5%). HR EI-MS found (calcd) for $\text{C}_{18}\text{H}_{25}\text{Cl}_2\text{N}_5\text{Ti}$: m/z 429.0974 (429.0966). Anal. Found (calcd) for $\text{C}_{18}\text{H}_{25}\text{Cl}_2\text{N}_5\text{Ti}$: C, 50.4 (50.3); H, 6.0 (5.9); N, 16.2 (16.3).

Ti(NNPh₂)Cl₂{HC(Me₂pz)₃} (9). A solution of HC(Me₂pz)₃ (0.37 g, 1.28 mmol) in benzene (20 mL) was added to a stirred

solution of $\text{Ti}(\text{NNPh}_2)\text{Cl}_2(\text{HNMe}_2)_2$ (**1**) (0.50 g, 1.28 mmol) in benzene (20 mL) over 15 min. The mixture was left to stir for a further 3 h, after which the solution was a blue-green color and some precipitate was present. The volume of solvent was reduced to approximately 20 mL under reduced pressure, and the mixture was left to stand for a further 2 h. The supernatant was decanted to yield **9** as a yellow-green powder which was dried in vacuo. Yield: 0.61 g (80%). ¹H NMR (CD₂Cl₂, 500.0 MHz): δ 7.93 (1H, s, *apical H*), 7.28 (4H, m, *ortho-H*), 7.13 (4H, m, *meta-H*), 6.88 (2H, m, *para-H*), 6.04 (2H, s, 4-*pz* H_{cis}), 5.89 (1H, s, 4-*pz* H_{trans}), 2.63 (3H, s, 3-*pz* Me_{trans}), 2.62 (6H, s, 5-*pz* Me_{cis}), 2.48 (3H, s, 5-*pz* Me_{trans}), 2.21 (6H, s, 3-*pz* Me_{cis}). ¹³C-¹H NMR (CD₂Cl₂, 125.8 MHz): δ 157.1 (3-*pz*_{trans}), 156.7 (3-*pz*_{cis}), 145.0 (*ipso-C*), 140.3 (5-*pz*_{cis}), 138.7 (5-*pz*_{trans}), 129.7 (*ortho-C*), 123.0 (*para-C*), 120.1 (*meta-C*), 109.3 (4-*pz*_{trans}), 108.9 (4-*pz*_{cis}), 68.5 (*apical-C*), 15.6 (3-*pz* Me_{cis}), 15.4 (3-*pz* Me_{trans}), 11.8 (5-*pz* Me_{cis}), 11.4 (5-*pz* Me_{trans}). IR (NaCl plates, Nujol mull, cm⁻¹): ν 1594 (br, w), 1305 (w), 1260 (m), 1092 (br, w), 1020 (br, w), 803 (m), 722 (m). EI-MS: m/z 503 $[\text{M} - \text{Me}_2\text{pz}]^+$ (7%), 203 $[\text{HC}(\text{Me}_2\text{pz})_2]^+$ (3%), 96 $[\text{Me}_2\text{pz}]^+$ (23%). Anal. Found (calcd) for $\text{C}_{28}\text{H}_{32}\text{Cl}_2\text{N}_8\text{Ti}$: C, 56.0 (56.1); H, 5.3 (5.4); N, 18.8 (18.7).

Ti(NNPh₂)Cl₂{HC(ⁿBupz)₃} (10). A solution of HC(ⁿBupz)₃ (0.19 g, 0.50 mmol) in benzene (15 mL) was added to a stirred solution of $\text{Ti}(\text{NNPh}_2)\text{Cl}_2(\text{HNMe}_2)_2$ (**1**) (0.20 g, 0.50 mmol) in benzene (20 mL) over 10 min. The solution was left to stir for 16 h, and the volatiles were then removed under reduced pressure to give **10** as a bright green powder. Yield: 0.28 g (81%). ¹H NMR (CD₂Cl₂, 500.0 MHz, 298 K): δ 10.13 (1H, s, *apical H*), 8.52 (2H, s, 5-*pz* H_{cis}), 8.32 (1H, s, 5-*pz* H_{trans}), 7.71 (2H, s, 3-*pz* H_{cis}), 7.60 (1H, s, 3-*pz* H_{trans}), 7.40 (4H, m, *ortho-H*), 7.24 (4H, m, *meta-H*), 6.98 (2H, m, *para-H*), 2.28 (6H, app t, 4-*pz*-CH₂CH₂CH₂CH₃), 1.38 (6H, m, 4-*pz*-CH₂CH₂CH₂CH₃), 1.23 (6H, m, 4-*pz*-CH₂CH₂CH₂-CH₃), 0.82 (9H, m, 4-*pz*-CH₂CH₂CH₂CH₃). ¹³C-¹H NMR (CD₂-Cl₂, 125.8 MHz): δ 146.3 (3-*pz*_{trans}), 144.8 (3-*pz*_{cis}), 143.6 (*ipso-C*), 129.3 (*ortho-C*), 123.5 (*para-C*), 123.4 (5-*pz*_{cis}), 123.1 (5-*pz*_{trans}), 119.5 (*meta-C*), 118.0 (4-*pz*_{cis}), 117.8 (4-*pz*_{trans}), 75.3 (*apical-C*), 32.9 (4-*pz*-CH₂CH₂CH₂CH₃_{trans}), 32.7 (4-*pz*-CH₂CH₂CH₂CH₃_{cis}), 32.7 (4-*pz*-CH₂CH₂CH₂CH₃_{trans}), 23.7 (4-*pz*-CH₂CH₂CH₂CH₃_{cis}), 22.7 (4-*pz*-CH₂CH₂CH₂CH₃_{trans}), 22.7 (4-*pz*-CH₂CH₂CH₂CH₃_{cis}), 13.9 (4-*pz*-CH₂CH₂CH₂CH₃_{cis}), 13.9 (4-*pz*-CH₂CH₂CH₂CH₃_{trans}). IR (NaCl plates, Nujol mull, cm⁻¹): ν 1595 (br, w), 1260 (w), 1091 (br, w), 1021 (br, w), 805 (w), 722 (w). Anal. Found (calcd) for $\text{C}_{34}\text{H}_{44}\text{Cl}_2\text{N}_8\text{Ti}$: C, 59.7 (59.8); H, 6.4 (6.5); N, 16.2 (16.4).

Alternative Syntheses of *fac*-N₃ Donor-Supported Hydrazido Complexes. Complexes **7**, **8**, **9**, and **10** were synthesized on the NMR tube scale from $[\text{Ti}(\text{NNPh}_2)\text{Cl}_2(\text{py})_2]_n$ (**4**) using the following general method. A solution of the *fac*-N₃ donor ligand (12.0 μmol) in C₆D₆ (0.2 mL) was added to a solution of **4** (5 mg, 10.8 μmol) in C₆D₆ (0.2 mL). A solid immediately precipitated out of the reaction mixture. The volatiles were removed under reduced pressure and the sample redissolved in CD₂Cl₂. Analysis by ¹H NMR indicated that in all cases the reaction had occurred cleanly to give the desired product.

Attempted Reaction of Ti₂(μ - η^2 , η^1 -NNMe₂)₂Cl₄(py)₂ (2) and Ti₂(μ - η^2 , η^1 -NNMe₂)₂Cl₄(HNMe₂)₂ (3) with Me₃[9]aneN₃, Me₃[6]aneN₃, HC(Me₂pz)₃, and HC(ⁿBupz)₃. A solution of the *fac*-N₃ donor ligand (25 μmol) in CD₂Cl₂ (0.2 mL) was added to a solution of **2** or **3** (25 μmol) in CD₂Cl₂ (0.2 mL). After 5 days of heating at 70 °C, analysis by ¹H NMR showed that in all cases only a mixture of the starting materials were present.

Table 8. Crystal Data Collection and Processing Parameters for $\text{Ti}_2(\mu\text{-}\eta^2,\eta^1\text{-NNMe}_2)_2\text{Cl}_4(\text{HNMe}_2)_2$ (**2**), $\text{Ti}_2\{\mu\text{-}\eta^2,\eta^1\text{-NN}(\text{CH}_2)_5\}_2\text{Cl}_4(\text{HNMe}_2)_3\cdot\text{C}_6\text{H}_6$ (**3**· C_6H_6), $\text{Ti}_2(\mu\text{-}\eta^2,\eta^1\text{-NNMe}_2)_2\text{Cl}_4(\text{py})_2$ (**5**), and $\text{Ti}(\text{NNPh}_2)\text{Cl}_2\{\text{HC}(\text{Me}_2\text{pz})_3\}_2\cdot 2\text{C}_6\text{H}_6$ (**9**· $2\text{C}_6\text{H}_6$)

	2	3 · C_6H_6	5	9 · $2\text{C}_6\text{H}_6$
empirical formula	$\text{C}_8\text{H}_{26}\text{Cl}_4\text{N}_6\text{Ti}_2$	$\text{C}_{27}\text{H}_{47}\text{Cl}_4\text{N}_7\text{Ti}$	$\text{C}_{14}\text{H}_{22}\text{Cl}_4\text{N}_6\text{Ti}_2$	$\text{C}_{40}\text{H}_{44}\text{Cl}_2\text{N}_8\text{Ti}$
fw	443.95	647.27	511.98	755.65
temp (K)	150	150	150	150
wavelength (Å)	0.71073	0.71073	0.71073	0.71073
space group	$P 2_1/n$	$P 2_1/c$	$C 2/c$	$P\bar{1}$
<i>a</i> (Å)	8.9547(2)	10.5306(2)	15.2735(4)	9.6913(2)
<i>b</i> (Å)	14.4471(3)	17.0858(3)	9.9708(3)	13.9790(3)
<i>c</i> (Å)	15.0142(4)	17.9110(3)	14.6349(4)	14.1852(3)
α (deg)	90	90	90	80.3636(9)
β (deg)	94.5104(9)	103.6204(7)	90.6119(13)	88.1593(9)
γ (deg)	90	90	90	86.2151(11)
<i>V</i> (Å ³)	1936.36(8)	3131.98(10)	2228.61(11)	1890.05(7)
<i>Z</i>	4	4	4	2
<i>d</i> _{calcd} (Mg m ⁻³)	1.523	1.373	1.526	1.328
abs coeff (mm ⁻¹)	1.375	0.875	1.207	0.408
R indices	0.0310, 0.0357	0.0329, 0.0369	0.0581, 0.0484	0.0390, 0.0452
<i>R</i> ₁ , <i>R</i> _w [<i>I</i> > 3σ(<i>I</i>)] ^a				

$$^a R_1 = \sum ||F_o| - |F_c|| / \sum |F_o|. R_w = \{ \sum w (|F_o| - |F_c|)^2 / \sum w |F_o|^2 \}^{1/2}.$$

Crystal-Structure Determination of $\text{Ti}_2(\mu\text{-}\eta^2,\eta^1\text{-NNMe}_2)_2\text{Cl}_4(\text{HNMe}_2)_2$ (2**), $[\text{Ti}_2\{\mu\text{-}\eta^2,\eta^1\text{-NN}(\text{CH}_2)_5\}_2\text{Cl}_4(\text{HNMe}_2)_3\cdot\text{C}_6\text{H}_6$ (**3**· C_6H_6), and $\text{Ti}_2(\mu\text{-}\eta^2,\eta^1\text{-NNMe}_2)_2\text{Cl}_4(\text{py})_2$ (**5**) and $\text{Ti}(\text{NNPh}_2)\text{Cl}_2\{\text{HC}(\text{Me}_2\text{pz})_3\}_2\cdot 2\text{C}_6\text{H}_6$ (**9**· $2\text{C}_6\text{H}_6$).** Crystal data collection and processing parameters are given in Table 8. Crystals were mounted on a glass fiber using perfluoropolyether oil and cooled rapidly to 150 K in a stream of cold N_2 using an Oxford Cryosystems CRYOSTREAM unit. Diffraction data were measured using an Enraf-Nonius KappaCCD diffractometer, and intensity data were processed using the DENZO–SMN package.³⁵ The structures were solved using SIR92³⁶ which located all non-hydrogen atoms. Subsequent full-matrix least-squares refinement was carried out using the CRYSTALS program suite.³⁷ Coordinates and anisotropic thermal parameters of all non-hydrogen atoms were refined. Carbon-bound hydrogen atoms were positioned geometrically. Nitrogen-bound hydrogens in **2** and **3**· C_6H_6 were located from Fourier difference maps and isotropically refined (for the purposes of estimating N–H···Cl hydrogen bonding parameters in Tables 1 and 2 geometrically positioned (N–H = 0.87 Å) atoms were used). Weighting schemes were applied as appropriate. Full listings of atomic coordinates, bond lengths and angles, and displacement parameters have been deposited at the Cambridge Crystallographic Data Centre.

Density Functional Theory Calculations. DFT calculations were carried out using the Amsterdam Density Functional program suite ADF 2002.02.³⁸ The generalized gradient approximation was employed, using the local density approximation of Vosko, Wilk, and Nusair,³⁹ together with nonlocal exchange correction by Becke⁴⁰

and nonlocal correlation corrections by Perdew.⁴¹ TZP basis sets were used with triple- ζ accuracy sets of Slater-type orbitals and a polarization function added to the main group atoms. The cores of the atoms were frozen up to 1s for C and N and 2p for Ti and Cl. Fragment analyses use the MOs of the chosen fragments as the basis set for the molecular calculation. Initial spin-restricted calculations are carried out on the fragments with the geometry that they have in the molecule; thus, the fragments are in a prepared singlet state. Neutral fragments were chosen as this assisted in drawing up the MO diagrams.

Acknowledgment. This work was supported by funding from the EPSRC and Rhodes Trust. Calculations were carried out using the facilities of the Oxford Supercomputing Centre.

Supporting Information Available: X-ray crystallographic files in CIF format for the structure determination of compounds **2**, **3**, **5**, and **9** and optimized geometries in Cartesian (*xyz*) form for compounds **I**, **II**, **III**, and **2**. This material is available free of charge via the Internet at <http://pubs.acs.org>.

IC051271J

(35) Otwinowski, Z.; Minor, W. *Methods Enzymol.* **1997**, *276*, 307.

(36) Altomare, A.; Cascarano, G.; Giacovazzo, G.; Guagliardi, A.; Burla, M. C.; Polidori, G.; Camalli, M. *J. Appl. Crystallogr.* **1994**, *27*, 435.

(37) Watkin, D. J.; Prout, C. K.; Carruthers, J. R.; Betteridge, P. W.; Cooper, R. I. *CRYSTALS*, version 11; Chemical Crystallography Laboratory: Oxford, UK, 2001.

(38) Baerends, E. J.; Autschbach, J. A.; Berces, A.; Bo, C.; Boeringer, P. M.; Cavallo, L.; Chong, D. P.; Deng, L.; Dickson, R. M.; Ellis, D. E.; Fan, L.; Fischer, T. H.; Fonseca Guerra, C.; Van Gisbergen, S. J. A.; Groeneveld, J. A.; Gritsenko, O. V.; Grüning, M.; Harris, F. E.; van den Hoek, P.; Jacobsen, H.; van Kessel, G.; Kootstra, F.; Vanlenthe, E.; Osinga, V. P.; Patchkovskii, S.; Phillipsen, P. H. T.; Post, D.; Pye, C. C.; Ravenek, W.; Ros, P.; Schipper, P. R. T.; Schreckenbach, G.; Snijders, J. G.; Sola, M.; Swart, M.; Swerhone, D.; te Velde, G.; Vernooijs, P.; Versluis, L.; Visser, O.; van Wezenbeek, E.; Wiesenekker, G.; Wolff, S. K.; Woo, T. K.; Ziegler, T. *Scientific Computing and Modelling NV*; Vrije Universiteit: Amsterdam, 2002.

(39) Vosko, S. H.; Wilk, L.; Nusair, M. *Can. J. Phys.* **1980**, *58*, 1200.

(40) (a) Becke, A. D. *Phys. Rev. A: At., Mol., Opt. Phys.* **1988**, *38*, 3098. (b) Becke, A. D. *J. Chem. Phys.* **1988**, *88*, 1053.

(41) Perdew, J. P. *Phys. Rev. B* **1986**, *33*, 8800.